PHOTON PRODUCTION BY SECONDARY NUCLEAR FUSION REACTIONS IN A LASER-DRIVEN PLASMA

A Thesis

Presented to

The Graduate School of

Addis Ababa University

In Partial Fulfillment of

The Requirement for the Degree of

Master of Science in Physics

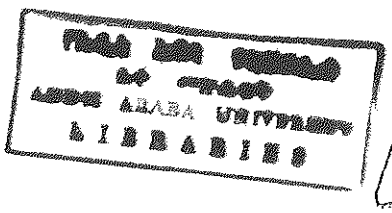

By

Takele Seda

June 1994

Addis Ababa

Tak
PHY
1994

DEDICATION

This thesis is dedicated to my mother W/o Saba Zegeye

Acknowledgments

I am greatly indebted to my advisor, Dr. S. S. Kotelnikov, for his generous advice, devotion and considerable encouragement, above all for his advice in creating computer program for the numerical simulation.

I wish to express my thanks to the Department of Physics for allowing me to use the computer for typing. I deliver my special thanks to Dr. S. Tesch who permitted me to use his computer for numerical simulation, and also to Dr. G. Gribakin from the University of South Wales, Australia who helped me by sending a copy of some books.

Also I am indebted to several relatives of mine Mulunesh Belay, Saba Zegeye, Mekonnen Dechassa, Tadesse Seda, Zerihun Belay and colleagues Desta Moges, Aynalem H/Michael, Almaz Abebe, Tesfaye Kassa and the others for their precious cooperation in meeting my requests while I was 33preparing the manuscript.

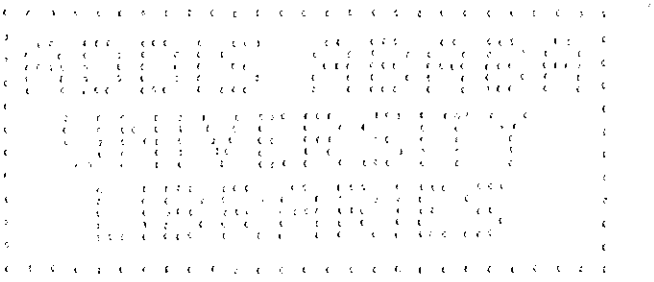

Abstract

Some aspects of the problem of a numerical simulation of rates and spectra of thermonuclear reaction products in a laser driven plasma are considered. Monte-Carlo simulation is the most commonly used method for this purpose. By using the properties of the analytical model it is proved that the problem can be reduced to the numerical solution of transcendential equation and numerical integration and the problem could be performed on a personal computer. The spectra of charged particles and secondary photons predicted by S. S. Kotelnikov and E. A. Choban [6] are discussed. The results are qualitatively in agreement with those determined experimentally and by use of the Monte-Carlo method. The proposed method of solution could be of use as additional tool for testing the model of the state of the laser target.

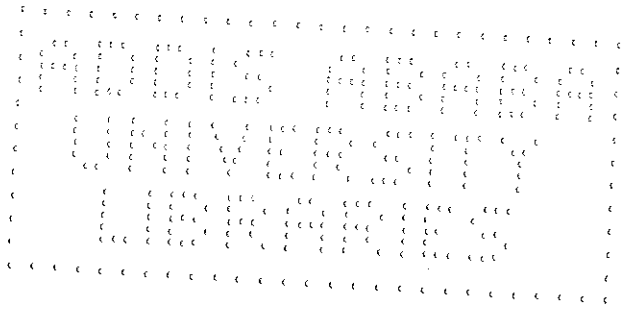

Table of contents.

INTRODUCTION

In both the lightest and heaviest nuclei, the mean binding energy per nuclear particle is less than it is in those of intermediate mass number. Consequently, it should be possible , in principle, to obtain nuclear energy either by fission of nuclei of the heaviest elements or by fusion of the lightest ones, the product in each case being nuclei in the intermediate mass range.

Controlled fusion is much more difficult to realize than the self sustained explosion reactions. The difficulties arise due to the fact that a sufficient energy gain in controlled fusion requires heating of a concentrated plasma (target) to a very high temperature $T \geq 10^8$ K and confining this plasma in such a state for a sufficiently long time τ witin the volume of the thermonuclear reactor.The confinement time is determined by the energy content of the plasma, and by the energy losses due to heating of walls, neutron emission, electron bremsstrahlung etc. The smaller the losses, the longer the confinement time. The reaction intensity is determined by the product $n\tau$ (called confinement parameter), the higher the plasma density the shorter the time required for a given number of nuclei to interact.

For the energy released in a thermonuclear reactor to exceed the energy consumed, Lawson's criterion must be satisfied. This criterion involves a definite combination of confinement parameter $n\tau$ and temperature T.

The problem of obtaining controlled fusion reactions can in principle be solved in four ways

i. prolonged heating of a dense ($n \geq 10^{15} cm^{-3}$) deuterium-tritium plasma in a reactor at a temperature about 10^8K.

ii. superfast (about 10^{-9} s) heating (inertial fusion) of very small volume of condensed thermonuclear materials (by electron beams, laser beams etc.)

iii. μ – *catalysis* and

iv. hybrid atomic-thermonuclear reactor.

Confinement by inertia has been verified by the thermonuclear explosions. Using an explosive nuclear fission reaction of the type A-bomb, the released energy is so high that it heats and compresses solid material with light nuclei so fast that the subsequent expansion and cooling is slow enough and much more energy is being released from the fusion reaction than one had to put by the fission reaction for ignition. After this well demonstrated success of the uncontrolled (explosive) inertial confinement fusion, the current aim is to simulate this process in a controlled way by using pulses of laser energy or of intense particle beams for ignition of the fusion reaction.

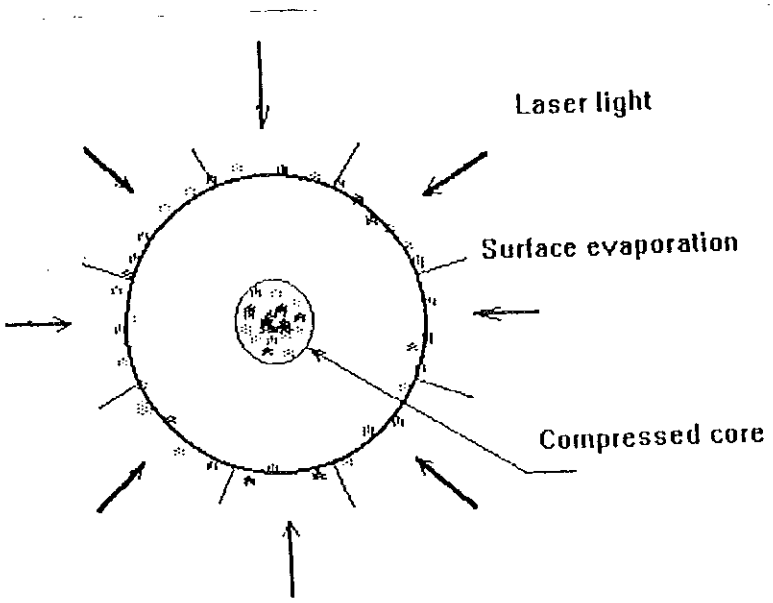

Fig. a. *The inertial fusion process. The target (pellet) is heated by incident laser or particle radiation, the full pellet is compressed by ablation of the hot surface material and finally full compression and ignition of the full pellet takes place.*

Some potential applications of inertially confined fusion other than nuclear weapons include

a. laboratory astrophysics of stellar interiors.

b. inertially-confined fusion reactors for pulsed energy production.

c. fusion reactors for civil power-plant applications.

The mechanism of inertially-confined fusion is illustrated in Fig. a. Rapid heating of the surface of a pellet (target) containing a mixture of hydrogen isotopes, or possibly other fusionable fuels, causes it to be compressed up to 10^3 times its solid state density and heated to fusion temperatures, approximately 10 keV (for a D-T mixture).

Since magnetic fields are not required, inertial confinement can proceed without any of the instability and anomalous transport mechanisms encountered in magnetic confinement. As a result it was once thought that inertial confinement might be the fastest route to fusion.

The interest in lasers as a possible source of energy arises from the characteristics of pulsed energy released from a fuel target with no external containment for which the time available for thermonuclear reactions is determined by the time required for hydrodynamical motion in the pellet.

Crude considerations show that the time required for laser-driven fusion [Ref. 24 &25], is of the order of 10^{-9} s and the energy in the range of tens of kilojoules, giving a power requirement of millions of megawatts. In order to prevent the plasma from spreading out and to ensure effective compression, the pulsed heating should be carried out simultaneously from all sides.

Once the target is heated to the fusion temperature, particles within the target duplicate themselves (self heating), so that no external devices for particle diagnosis are necessary as in the other inertial confinements. Thus, in addition to fusion energy production, laser-driven fusion reactions are advantageous for corpuscular diagnostics. specially for the investigation of particles in a compressed region with number density (concentration) up to about 10^{24} cm^{-3}.

The theoretical and computational results reviewed in this paper predicts that the spectrum and thereby the yield of the particles (neutron and photon) obtained permit us to investigate different models of states of compressed targets in a laser-driven fusion.

The thesis has been divided into four chapters. In chapter one, we reviewed certain aspects of the laser-driven fusion reactions (primary and secondary) arerevised and analytical calculations are developed for the rate and spectrum of particles produced in the reactions (see Fig. (b). below).

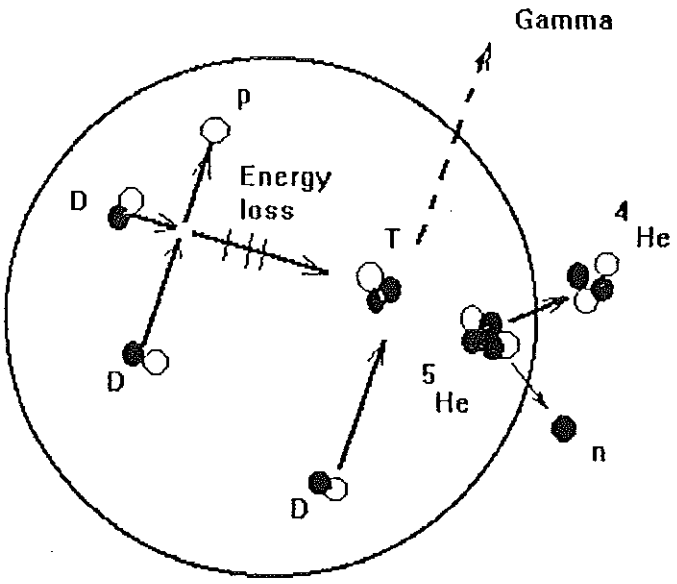

Fig.(b.) *Secondary DT nuclear fusion reaction. Primary DD reactions produce 1 MeV tritons, reacting again with remainder deuterons to produce secondary DT photons.*

The distributions of particles produced in the secondary fusion reactions and their propagation in the plasma (their interaction with the plasma particles) is governed by the Fokker-Planck equation. This is discussed in chapter two with the help of the Green function method. Results in chapters one and two are analytical. The possible sources of charged particles and the influences on their propagation within the target plasma which arises from the interactions with the plasma particles are discussed in chapter two.

The basic characteristics of computer methods for solving the problem are given in chapter three. It provides the algorithm and block structure of the numerical program. The results of the numerical calculation are presented schematically in chapter four. The possiblities of detecting secondary photons is also discussed.

CHAPTER ONE

1. NUCLEAR FUSION REACTIONS IN D-T TARGETS

Fusion reactions occur when the isotopes of light elements combine to form two or more reaction products, each different from the initial fuels.

Nuclear fusion reaction may be written in the following manner [Ref. 1]

$$A + B \rightarrow C + D + ..., \quad (Q) \qquad (1.1)$$

where A and B are the two fuels or reactants, C and D are reaction products and Q is the total energy released by the reaction, usually expressed in MeV. It is generally true that at a given temperature, reactions involving the nuclei of hydrogen isotopes take place readily under the Coulomb barrier repulsion (called sub-barrier reaction or barrier penetration). Among the isotopes of hydrogen, reactions with deuterium and tritium provide considerable net gain of energy due to their higher reaction cross-section.

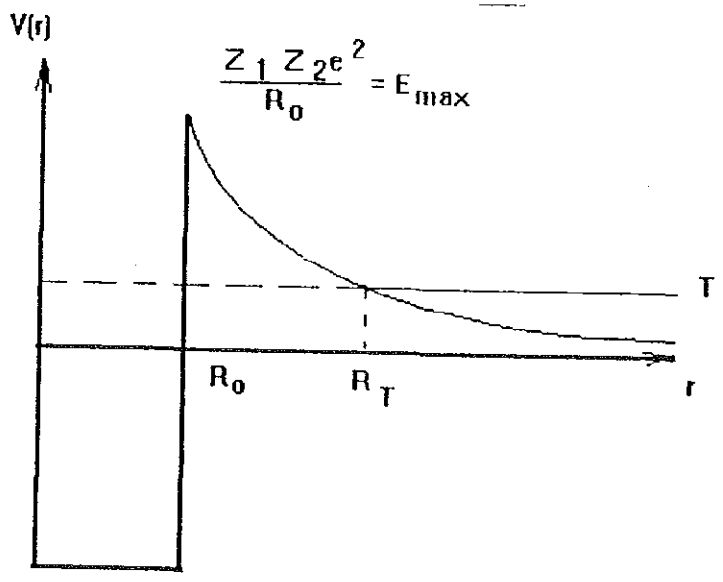

Fig. 1.1 *Variation of Coulomb potential energy with distance between nuclei (square well nuclearpotential is consider)*

Figure 1.1 is a schematic of potential energy barrier between two nuclei. When they are a great distance apart, they feel only the Coulomb force. They must overcome this large potential energy barrier in order for their centre of masses to approach within an effective nuclear diameter, Ro. Within Ro , the attractive nuclear force comes in to play, and nuclear reaction proceeds.

According to classical theory, the energy which must be supplied to the nuclei to surmount the Coulomb barrier, i.e. the maximum energy required to overcome the electrostatic repulsion so that fusion can occur is given by

$$E_{\max} = \frac{Z_1 Z_2 e^2}{R_o} \qquad (1.2)$$

where Z_1 and Z_2 are the respective charges (or atomic numbers) of the reacting nuclei.

The energy required to overcome the Coulomb barrier must come from the kinetic energy (T) of the reacting nuclei. For a characteristic nuclear diameter $5 \times 10^{-13} cm$, the height of the Coulomb barrier is

$$E_{\max} = 0.28 Z_1 Z_2 \quad \text{MeV} \qquad (1.3)$$

Although energies of the order of magnitude indicated by equation (1.3) must be supplied to nuclei to cause them to combine fairly rapidly, a significant fusion reactions occur when the relative energies of the reactants are less than those corresponding to the top of the Coulomb barrier. In other words, there is no threshold energy determined by the maximum electrostatic repulsion of the interacting nuclei, below which the fusion reaction will not occur. Fusion reactions are quantum mechanical processes, and it is possible for a pair of reactants with energies less than $E_{\max}$ to tunnel through the potential barrier indicated in Fig. 1.1 and form a compound nucleus. This quantum mechanical process (the penetration probability for two nuclei to combine) for nuclear fusion reaction at low energies [Ref. 2], is proportional to the Gamow factor which is given by

$$D = \exp\left\{-\frac{4\pi^2 Z_1 Z_2 e^2}{hu}\right\} \qquad (1.4)$$

where h is Planck's constant and u is the relative velocity of the reacting nuclei.

1.1 PRIMARY FUSION REACTIONS IN D-T TARGETS

Several experiments have been done to measure the ion temperature from the spectra of particles produced in a laser-driven fusion, [Ref. 3, 4] using the time of flight technique. These experiments show that thermal broadening of the energy spectra of the emitted particles (especially neutron) during the fusion cause a dependence of the particle line width on the ion temperature.

The ion density and temperature can be determined using the particle diagnostics by the primary reaction products which in the case of D-T targets include [Ref. 5]

$D + D \rightarrow {}^3H_e + n$	Q = 3.27 MeV	(1.1.1)
$D + D \rightarrow T + p$	Q = 4.03 MeV	(1.1.2)
$D + T \rightarrow {}^4H_e + n$	Q = 17.6 MeV	(1.1.3)
$D + T \rightarrow {}^5H_e + \gamma$	Q = 16.63 MeV	(1.1.4)
$T + T \rightarrow {}^4H_e + 2n$	Q = 11.33 MeV	(1.1.5)
$T + T \rightarrow {}^5H_e + n$	Q = 16.02 MeV	(1.1.6)

1.2 SECONDARY FUSION REACTIONS IN D-T TARGETS

Fast charged particles which are produced as a result of the primary fusion reactions can react with the original D or T. Such fusion reactions are referred to as [Ref. 6] secondary fusion reactions. The point is that charged particles formed in primary reactions slow down in the target plasma, and, as a result the rate and spectra of the particles in the secondary reactions depend on the slowing-down length (stopping power), which is a function of the electron density and temperature.

Measurement of the spectra and rate of the secondary reaction products and comparison with calculated results can provide us with information about the density and temperature of electrons of the plasma.

It is interesting to consider the following secondary reactions in the D-T case, with charged particles p, T and ^3He formed in the primary reactions.

$p + D \rightarrow {}^3He + \gamma$	Q = 6.49 MeV	(1.2.1)
$p + T \rightarrow {}^4He + \gamma$	Q = 19.81 MeV	(1.2.2)
$T + D \rightarrow {}^5He + \gamma$	Q = 16.63 MeV	(1.2.3)
$^3He + D \rightarrow {}^4He + p$	Q = 18.35 MeV	(1.2.5)
$^3He + D \rightarrow {}^5L_i + \gamma$	Q = 16.39 MeV	(1.2.6)
$T + D \rightarrow {}^4He + n$	Q = 17.6 MeV	(1.2.4)
$^3He + T \rightarrow {}^5He + p$	Q = 11.14 MeV	(1.2.7)
$^3He + T \rightarrow {}^4He + p + n$	Q = 12.10 MeV	(1.2.8)
$^3He + T \rightarrow {}^4He + D$	Q = 14.32 MeV	(1.2.9)

1.3 THE REACTION RATE AND SPECTRUM OF MASSIVE PARTICLES FROM PRIMARY FUSION REACTIONS

When nuclei are sufficiently energetic, they participate in thermonuclear reactions. For a Maxwellian two-particle distribution, the probability that a particle is inside a three dimensional volume element d^3u is

$$f(\vec{u})\, d^3u = \left(\frac{\mu}{2\pi\Theta}\right)^{3/2} \exp\left(-\frac{\mu u^2}{2\Theta}\right) d^3u \qquad (1.3.1)$$

where μ is the reduced mass of the pair, Θ is the temperature (in energy units) and $\vec{u}$ is the relative velocity of the pair. (The centre of mass motion has been factored out by the Jacobean transformation of the velocities of the two particles to the velocity of the centre of mass and the velocity of the pair), [Ref. 7]. The reaction rate is then

$$\frac{dN}{dt} = n_1 n_2 \int \sigma(u)\, u f(\vec{u}) d^3u = n_1 n_2 \, \langle \sigma u \rangle \qquad (1.3.2)$$

where n_1 and n_2 are the number densities of the reacting particles, $\sigma(u)$ is the cross-section for the reaction as a function of the relative velocity and N the concentration of particles produced in the reaction.

Now let us take one of the primary fusion reactions (equation 1.1.3) and find the reaction rate and the spectrum of the neutrons produced. The rate equation for this D-T reaction is

$$\frac{dN_n}{dt} = n_D n_T \int f(\vec{V}) d^3V \int f(\vec{u}) \sigma(u) u d^3u \qquad (1.3.3)$$

where $\vec{V}$ is the velocity of the centre of mass and f(v) is its distribution function (the integral being over the volume of the velocity space).

In all nuclear reactions, the total energy and momentum are conserved quantities. The necessity for conserving the total linear momentum in a nuclear reaction suggests that the kinematical description be in terms of the motion of the centre of mass of the nuclear system plus the motion of the particles relative to their centre of mass co-ordinate system.

The conservation of energy in the centre of mass co-ordinate system implies that

$$\frac{m_n v_{nc}^2}{2} + \frac{m_\alpha v_{\alpha c}^2}{2} = \frac{\mu u^2}{2} + Q \qquad (1.3.4)$$

and momentum conservation in the centre of mass co-ordinate system gives

$$m_n \vec{v}_{nc} + m_\alpha \vec{v}_{\alpha c} = 0 \qquad (1.3.5)$$

where $\vec{v}_{nc}$ and $\vec{v}_{\alpha c}$ are the velocities of neutron and alpha particle respectively in the centre of mass system. Solving for $\vec{v}_{\alpha c}$ from (1.3.5) and using it in (1.3.4), one obtains for the square of the velocity of neutron in the centre of mass system

$$v_{nc}^2 = \frac{2}{m_n}\left\{\frac{m_\alpha}{m_n + m_\alpha}\left(\frac{\mu u^2}{2} + Q\right)\right\} \qquad (1.3.6)$$

Then the reaction rate can be written as

$$\frac{dN_n}{dt} = n_D n_T \int f(\vec{V}) d^3V \int f(\vec{u}) \sigma(u) u\, d^3u \int dv_{nc}^2 \delta(v_{nc}^2 - \varphi(u)) \qquad (1.3.7)$$

where $\delta(v_{nc}^2 - \varphi(u))$ is the delta function and $\varphi(u) = \frac{2}{m_n}\left\{\frac{m_\alpha}{m_n + m_\alpha}\left(\frac{\mu u^2}{2} + Q\right)\right\}$

Using $\int \frac{d\sigma(u)}{d\Omega} d\Omega$ for $\sigma(u)$ and $\frac{2v_{nc}^2 dv_{nc}}{v_{nc}}$ for dv_{nc}^2, we obtain

$$\frac{dN_n}{dt} = \frac{n_D n_T}{2\pi} \int f(\vec{V}) d^3V \int f(\vec{u}) \sigma(u)\, u\, d^3u \int \frac{d^3 v_{nc}}{v_{nc}} \delta(v_{nc}^2 - \varphi(u)) \qquad (1.3.8)$$

where $d^3 v_{nc} = dv_{nc}\, v_{nc}^2 d\Omega$ and the cross-section of low energy particles in the case of s-scattering, [Ref. 8] is isotropic so that $\frac{d\sigma(u)}{d\Omega} = \frac{\sigma(u)}{4\pi}$.

These integrals motivate us to use the Jacobean transformation of the velocity of the centre of mass to the velocities of neutron in the laboratory and in the centre of mass systems.

$$\vec{v}_{nl} = \vec{V} + \vec{v}_{nc} \qquad (1.3.9)$$

where $\vec{v}_{nl}$ is velocity of neutron in the laboratory system. The transformation is

$$d^3V d^3 v_{nc} = \left| \frac{\partial(\vec{V}, \vec{v}_{nc})}{\partial(\vec{v}_{nl}, \vec{v}_{nc})} \right| d^3 v_{nl} d^3 v_{nc} = d^3 v_{nl} d^3\, v_{nc} \qquad (1.3.10)$$

On substituting this into equation (1.3.8), we arrive at

$$\frac{dN_n}{dt} = \frac{n_D n_T}{2\pi} \int f(\vec{v}_{nl} - \vec{v}_{nc}) \int f(\vec{u})\, \sigma(u)\, u \int \frac{\delta(v_{nc}^2 - \varphi(u))}{v_{nc}} d^3 v_{nc}\, d^3 u\, dv_{nl}^3 \qquad (1.3.11)$$

But the distribution function of the centre of mass $f(\vec{V}) = f(\vec{v}_{nl} - \vec{v}_{nc})$ can be written as

$$f(\vec{v}_{nl} - \vec{v}_{nc}) = \left(\frac{M}{2\pi\Theta}\right)^{3/2} \exp\left\{-\frac{M}{2T}(v_{nl}^2 + v_{nv}^2 - 2v_{nl}v_{nc}\cos\theta)\right\} \qquad (1.3.12)$$

where $M = m_D + m_T$ is the total mass of the reacting nuclei and θ is the angle between the velocities of neutron in the laboratory and the centre of mass systems.

If we put $d^3 v_{nl} = v_{nl}^2 dv_{nl} d\Omega$ and perform the integral of equation (1.3.11) over the solid angle $d\Omega$ (only one term is a function of θ), the integral

$\int_o^{\pi}\int_o^{2\pi} \exp(\frac{M v_{nl} v_{nc} \cos\theta}{\Theta}) d\Omega$ becomes

$$\frac{4\pi\Theta}{M v_{nl} v_{nc}} \sinh(\frac{M v_{nl} v_{nc}}{\Theta}) \qquad (1.3.13)$$

Thus,

$$\frac{dN_n}{dt} = \frac{2 n_D n_T \Theta}{M} \{\int_o^{\infty} \left(\frac{M}{2\pi\Theta}\right)^{3/2} \exp[-\frac{M}{2\Theta}(v_{nl}^2 + v_{nc}^2] \sinh(\frac{M v_{nl} v_{nc}}{\Theta}) v_{nl}\, dv_{nl}$$

$$\times \int f(\vec{u})\, \sigma(u)\, u\, d^3u \int \frac{\delta(v_{nc}^2 - \varphi(u))}{v_{nc}^2} d^3 v_{nc} \} \qquad (1.3.14)$$

Using the property of delta function, [Ref. 9],

$$\delta(v_{nc}^2 - \varphi(u)) = \frac{\delta(v_{nc} - v_{nc}^{(o)})}{\left|\frac{d}{dv_{nc}}(v_{nc}^2 - \varphi(u))\right|_{v_{nc}=v_{nc}^{(o)}}} \qquad (1.3.15)$$

where $v_{nc}^{(o)}$ is the value of v_{nc} at $v_{nc}^2 - \varphi(u) = 0$.

The first term on the right hand side of equation (1.3.4) is very small (in the order of keV) in comparison with the second term (Q) which is in the order of MeV, hence it can be neglected. Therefore, equation (1.3.15), will become

$$\delta(v_{nc}^2 - \frac{2 m_\alpha Q}{m_n(m_n + m_\alpha)}) = \frac{\delta(v_{nc} - v_{nc}^{(o)})}{2 v_{nc}} \qquad (1.3.16)$$

with $v_{nc}^{(o)} = \left[\frac{2 m_\alpha Q}{m_n(m_n + m_\alpha}\right]^{1/2}$

Now the rate equation can be rewritten as

$$\frac{dN_n}{dt} = \frac{\Theta n_D n_T}{M} (\frac{M}{2\pi\Theta})^{3/2} \int_0^{\infty} \{\exp[-\frac{M}{2\Theta}(v_{nl}^2 + v_{nc}^2)] \sinh(\frac{M v_{nc} v_{nl}}{\Theta}) v_{nl}$$

$$\times \int f(\vec{u})\, \sigma(u)\, u\, d^3u \int \frac{\delta(v_{nc} - v_{nc}^{(o)})}{v_{nc}} d^3 v_{nc} \} dv_{nl} \qquad (1.3.17)$$

The integral $\int f(\vec{u})\,\sigma(u)\,u\,d^3u$ is simply the average value of the product $\sigma(u).u$ denoted by $\langle \sigma u \rangle$.

By the property of delta function, which is valid in any number of dimensions

$$\frac{dN_n}{dt} = \frac{\Theta n_D n_T}{M(v_{nc}^{(o)})}\left(\frac{M}{2\pi\Theta}\right)^{3/2}\langle \sigma u\rangle \int_0^{\infty} \frac{\exp\{-[\frac{M}{2\Theta}(v_{nl}-v_{nc}^{(0)})^2\}-\exp\{-[\frac{M}{2\Theta}(v_{nl}+v_{nc}^{(0)})\}^2}{2} v_{nl}\,dv_{nl} \qquad (1.3.18)$$

It was already seen that $\frac{\mu u^2}{2}$ is much smaller than Q, and hence

$(v_{nc}^{(0)})^2 = \frac{2m_\alpha}{m_n(m_n+m_\alpha)}Q$. Then $\frac{M}{2}(v_{nc}^{(0)})^2 = \frac{m_\alpha}{m_n}Q$ which is very much greater than Θ.

This implies that the second term under the integral is vanishing and the equation reduces to

$$\frac{dN_n}{dt} = \frac{\Theta n_D n_T}{2M(v_{nc}^{(0)})^3}\left(\frac{M}{2\pi\Theta}\right)^{3/2}\langle \sigma u\rangle \int \exp[-\frac{M}{2\Theta}(v_{nl}-v_{nc}^{(0)})^2]\,v_{nl}\,dv_{nl} \qquad (1.3.19)$$

From equation (1.3.19), the D-T neutron velocity spectrum can be obtained by changing the integral to differential equation as:

$$\frac{d^2N_n}{dt\,dv_{nl}} = \frac{\Theta n_D n_T}{2M(v_{nc}^{(0)})^3}\left(\frac{M}{2\pi\Theta}\right)^{3/2}\langle \sigma u\rangle\, v_{nl}\exp[-\frac{M}{2\Theta}(v_{nl}-v_{nc}^{(0)})^2] \qquad (1.3.20)$$

The D-T neutron spectrum is immediately obtainable by changing the variables from velocity to energy.

$v_{nl} = \sqrt{\frac{2E_n}{m_n}}$, so that $dv_{nl} = \frac{dE_n}{\sqrt{m_n E_n}}$ and $v_{nc}^{(0)} = \sqrt{\frac{2E_n}{m_n}}$

Then

$$\frac{d^2N_n}{dt\,dE_n} = \frac{n_D n_T}{2}\left(\frac{M m_n}{\Theta}\right)^{1/2}\frac{E_n}{(4\pi E_n^{(0)})^{3/2}}\langle \sigma u\rangle \exp[-\frac{M}{2\Theta}(\sqrt{\frac{2E_n}{m_n}}-\sqrt{\frac{2E_n^{(0)}}{m_n}})^2 \qquad (1.3.21)$$

By completing the square in the exponential

$$\frac{d^2N_n}{dt\,dE_n} = \frac{n_D n_T}{2}\left(\frac{M m_n}{\Theta}\right)^{1/2} \frac{E_n}{(4\pi E_n^{(0)})^{3/2}} \langle \sigma u \rangle \exp\{-\frac{M}{2\Theta}[\frac{(\frac{2E_n}{m_n} - \frac{2E_n^{(0)}}{m_n})^2}{(\sqrt{\frac{2E_n}{m_n}} + \sqrt{\frac{2E_n^{(0)}}{m_n}})^2}]\} \qquad (1.3.22)$$

Since the expressions in the exponential in the sum are under radicals, it is reasonable to assume that $E_n \approx E_n^{(0)}$. Therefore,

$$\frac{d^2N_n}{dt\,dE_n} = \frac{n_D n_T}{2}\left(\frac{M m_n}{\Theta}\right)^{1/2} \frac{E_n}{(4\pi E_n^{(0)})^{3/2}} \langle \sigma u \rangle \exp\{-\frac{M}{4m_n}\frac{(E_n - E_n^{(0)})^2}{\Theta E_n^{(0)}} \qquad (1.3.23)$$

This is the spectrum of primary neutron which is Gaussian having maximum value at $E_n = E_n^{(0)}$.

Equation (1.3.23) can be written as:

$$\frac{d^2N_n}{A\,dt\,dE_n} = \exp\{-\frac{M}{4m_n}\frac{(E_n - E_n^{(0)})^2}{\Theta E_n^{(0)}} \qquad (1.3.24)$$

with $A = \frac{n_D n_T}{2}\left(\frac{M m_n}{\Theta}\right)^{1/2} \frac{E_n}{(4\pi E_n^{(0)})^{3/2}} \langle \sigma u$

The half width of the spectrum can be found by equating equation (1.3.25) to 1/e which gives,

$$\frac{M}{4m_n}\frac{(\Delta E_n)^2}{\Theta E_n^{(0)}} = 1 \qquad (1.3.25)$$

Then the half width of the spectrum will be

$$\Delta E_n = [\frac{4m_n}{M} E_n^{(0)} \Theta]^{1/2} \qquad (1.3.26)$$

With known value of the ion temperature "Θ" from equation (1.3.26), the amplitude of the spectrum can be found immediately.

1.4 THE REACTION RATE AND SPECTRUM OF PHOTONS FROM PRIMARY FUSION REACTIONS

In the same way as we did in section (1.3), considering equation (1.1.4), the primary photon (γ-ray) rate of reaction per incident tritons with n_T atoms per unit volume into a solid angle $d\Omega$ of an element of target consisting n_D deuteron atoms per unit volume will be given by

$$\frac{dN_\gamma}{dt} = n_D n_T \int f(\vec{V})\, d^3V \int f(\vec{u})\, u\, \sigma(u)\, d^3u \qquad (1.4.1)$$

The integral with respect to the velocity of the centre of mass is simply

$$\int f(\vec{V})\, d^3V = \int f(\vec{V})\, V^2\, dV\, d\Omega \qquad (1.4.2)$$

where $d\Omega = d(-\cos\theta)\, d\varphi$ and θ is the angle between the velocity of the centre of mass ($\vec{V}$) and the momentum of photon in the centre of mass.

For a Maxwellian plasma

$$\int f(\vec{V})\, V^2\, dv\, d\Omega = \left(\frac{M}{2\pi\Theta}\right)^{3/2} \int \exp\left[-\frac{MV^2}{2\Theta}\right] V^2\, dV\, d\Omega \qquad (1.4.3)$$

Then the rate equation becomes

$$\frac{dN_\gamma}{dt} = n_D n_T \left(\frac{M}{2\pi\Theta}\right)^{3/2} \langle \sigma u \rangle \int \exp\left(-\frac{MV^2}{2\Theta}\right) V^2\, dV\, d\Omega \qquad (1.4.4)$$

In order to obtain the energy distribution of the photon, we must transform the variable from velocity to energy. This can be done via Lorentz transformation from the laboratory system to the centre of mass system of the photon energy which is

$$E_\gamma = (E'_\gamma + \vec{p}'_\gamma \cdot \vec{V}) \frac{1}{\sqrt{1-\frac{V^2}{c^2}}} \qquad (1.4.5)$$

where E_γ and E'_γ are energies of the photon in the laboratory and in the centre of

mass systems respectively and $\vec{p_\gamma'}$ is momentum of photon in the centre of mass system.

For non-relativistic particles, $\frac{1}{\sqrt{1-\frac{V^2}{c^2}}} \approx 1$, so that

$$E_\gamma = E_\gamma'(1 + \tfrac{V}{c}\cos\theta) \tag{1.4.6}$$

with $\frac{E_\gamma'}{c} = p_\gamma'$ and c is velocity of light . Multiplying equation (1.4.4) by

$\int \delta[E_\gamma - E_\gamma'(1 + \frac{V}{c}\cos\theta)]\, dE_\gamma$, we obtain

$$\frac{d^2N_\gamma}{dt\,dE_\gamma} = n_D n_T (\tfrac{M}{2\pi\Theta})^{3/2} \langle\sigma u\rangle \int \exp[-\tfrac{MV^2}{2\Theta}]$$

$$\text{x}\ \delta[E_\gamma - E_\gamma'(1 + \tfrac{V}{c}\cos\theta)]\, V^2\, dV d\Omega \tag{1.4.7a}$$

Since delta function is even, equation (1.4.7a) is equivalent to

$$\frac{d^2N_\gamma}{dt\,dE_\gamma} = n_D n_T (\tfrac{M}{2\pi\Theta})^{3/2} \langle\sigma u\rangle \int \exp[-\tfrac{Mv^2}{2\Theta}] \frac{V^2}{\left|\frac{E_\gamma'}{c}\cos\theta\right|} \delta[V - \frac{E_\gamma - E_\gamma'}{\frac{E_\gamma'}{c}\cos\theta}]\, dV d\Omega \tag{1.4.7b}$$

By the property of delta function this becomes

$$\frac{d^2N_\gamma}{dt\,dE_\gamma} = n_D n_T (\tfrac{M}{2\pi\Theta})^{3/2} \langle\sigma u\rangle \int \exp\{-\tfrac{Mc^2}{2\Theta}(\frac{E_\gamma - E_\gamma'}{E_\gamma'\cos\theta})^2\}(\frac{E_\gamma - E_\gamma'}{E\cos\theta})^2 \frac{c^3}{E_\gamma'|\cos\theta|} d \tag{1.4.8}$$

When the integral over $d\varphi$ is performed, equation (1.4.8) reduces to

$$\frac{d^2N_\gamma}{dt\,dE_\gamma} = 2\pi n_D n_T (\tfrac{M}{2\pi\Theta})^{3/2} \langle\sigma u\rangle \int_{-1}^{1} \exp\{-\tfrac{Mc^2}{2\Theta}(\frac{E_\gamma - E_\gamma'}{E_\gamma'})^2 \frac{1}{\cos^2\theta}\} x$$

$$\frac{c^3}{E_\gamma'|\cos\theta|}(\frac{E_\gamma - E_\gamma'}{E_\gamma'\cos\theta})^2 d(-\cos\theta) \tag{1.4.9}$$

Letting $y = -\frac{1}{\cos^2\theta}$

$$\frac{d^2N_\gamma}{dt\,dE_\gamma} = 2\pi\Theta n_D n_T \left(\frac{M}{2\pi\Theta}\right)^{3/2} \langle\sigma u\rangle \int_{\infty}^{1} \exp\left\{-\frac{Mc^2}{2\Theta}\left(\frac{E_\gamma - E_\gamma'}{E_\gamma'}\right)^2 y\right\} \frac{c^3}{E_\gamma'} \left(\frac{E_\gamma - E_\gamma'}{E_\gamma'}\right)^2 d \qquad (1.4.10)$$

When the integral is performed, we will arrive at the following energy spectrum of the photon

$$\frac{d^2N_\gamma}{dt\,dE_\gamma} = 2n_D n_T \frac{c}{E_\gamma'} \left(\frac{M}{2\pi\Theta}\right)^{1/2} \langle\sigma u\rangle \exp\left\{-\frac{Mc^2}{2\Theta}\left(\frac{E_\gamma - E_\gamma'}{E_\gamma'}\right)^2\right. \qquad (1.4.11)$$

which is Gaussian having maximum value at $E_\gamma = E_\gamma'$. The half width of the spectrum is the point at which the quantity $\frac{Mc^2}{2\Theta}\left(\frac{E_\gamma - E_\gamma'}{E_\gamma'}\right)^2$ equals unity. At this value, the width of the spectrum is

$$\Delta E_\gamma = \frac{E_\gamma'}{c}\left(\frac{2\Theta}{M}\right)^{1/2} \qquad (1.4.12)$$

From measured values of ΔE_γ and calculated values of Θ using equation (1.4.12), the amplitude of the spectrum $A = 2n_D n_T \sqrt{\frac{M}{2\pi\Theta}}\, \frac{c}{E_\gamma'} \langle\sigma u\rangle$ can be determined.

CHAPTER TWO

2. PROPAGATION OF CHARGED PARTICLES IN A HIGH-DENSITY PLASMA

As it has been discussed in section (1.2), charged particles which are the products of the primary fusion reactions in a plasma don't deposit locally where they were created. They can travel some distance before they are stopped and can undergo fusion reactions with the remainder targets to produce secondary fusion products.

When charged particles travel a given path length in a compressed fuel region [Ref. 10, 11] ,they suffer energy loss because of the Coulomb interactions with electrons and ions in the plasma. Charged particles of the environment plasma, close to the test particle act as a screen between the test particle and more distant charged particles. The length parameter that makes this transition is [Ref. 12] known as Debye length and is given by

$$\lambda_d = [\frac{\Theta}{4\pi n_e e^2}]^{1/2} \qquad (2.1)$$

where Θ is temperature of the plasma (in energy units) n_e is the number density of electrons and e is the electronic charge. Charged particles situated further than a Debye length from the test particle have a negligible effect on the trajectory of the test particle.

Plasma phenomena that takes place over distances greater than the Debye length cannot be described in terms of individual particle motion, but rather depend upon the collective motions of particles. The presence of multiple Coulomb collision in plasma particle interaction change the distribution (spectrum) of particles from its original Gaussian form in the primary reactions (see equations (1.3.24) and (1.4.11)).

The approach to the problem of treating changes in a distribution function resulting from frequently occurring events, each of which produces a small change in the momentum of a particle [Ref. 13, 14], is to use the Fokker-Planck equation.

2.1. THE FOKKER-PLANCK EQUATION

The problem of calculating the reaction rate and spectrum of charged particles produced in the primary reactions in a plasma while interacting with many other charged particles can be addressed by use of the Fokker-Planck equation.

In the derivation of the Fokker-Planck equation, it was assumed that the infinitesimal change of the velocity components with respect to the velocity ($\frac{|\Delta\vec{v}|}{v}$ <<1) are most probable and that in the change only terms up to the second order are important. The Fokker-Planck equation can be described [Ref. 15] as an equation that predicts the time evolution (up to and including the achievement of a steady state) of distribution function of one group of particles - the "test" particles - in Coulombic collisional interaction with another group -the "field" particles.

The Fokker-Planck equation can be written from Boltzmann kinetic equation in the following form for inertial confinement fusion reactions

$$\frac{\partial f}{\partial t} + \vec{v}.\frac{\partial f}{\partial \vec{r}} + \frac{\partial \vec{j}}{\partial \vec{v}} = S(\vec{v}, \vec{r}) \qquad (2.1.1)$$

where $\frac{\partial}{\partial \vec{r}}$ and $\frac{\partial}{\partial \vec{v}}$ are gradients with respect to the co-ordinate and velocity respectively, f is the distribution function for the test particles, S is the source of the particles which in our case is (see equations (1.3.24) and (1.4.11)) Gaussian and $\vec{j}$ represents the flux of particles in the velocity space. The components of $\vec{j}$ are given by

$$j_i = a_i(\vec{v})f + D_{ik}(\vec{v})\frac{\partial f}{\partial v_k} \qquad (2.1.2)$$

where $a_i(\vec{v})$ and $D_{ik}(\vec{v})$ are friction and diffusion coefficients respectively . The first term of the flux which has only one component parallel to $\vec{v}$, represents the dynamical friction, has influences in slowing down of particles having energies greater than the mean kinetic energy of the field particles by collision with these particles.The second term of the flux represents diffusion in velocity space. A steady state is reached when the dynamical friction (downward in energy for higher-energy particles) and diffusion (upward in energy for lower-energy particles) reach a balance, as modified by the presence of sources and sinks.The Fokker-Planck equation therefore, represents the effect of small-angle collisions in causing a continuous flow of points in velocity space, with the flux of particles being $\vec{j}$.

In nuclear fusion reactions, the interacting test particles produced in the primary reactions are fast particles having energies greater than the field particles. Therefore, the diffusion term in equation (2.1.2) is very small [$\frac{\left|D\frac{\partial f}{\partial \vec{v}}\right|}{\left|\vec{a}f\right|} \propto \frac{T}{E} << 1$] compared to the dynamical friction term. Hence it can be neglected and the Fokker-Planck equation will be reduced to

$$\frac{\partial f}{\partial t} + \vec{v}\frac{\partial f}{\partial \vec{r}} + \frac{\partial}{\partial \vec{v}}[\vec{a}(\vec{v})f] = S(\vec{v}) \qquad (2.1.3)$$

2.2 THE STOPPING POWER (FRICTION) COEFFICIENT

It has been discussed in the foregoing sections that fast ions (charged particles) in a plasma are stopped by interacting with the plasma, and lose their energy by transferring it to the interacting plasma particles. To find this retarding force, let the particles of the plasma moving with a velocity $\vec{v}'$ and charge $Z_1 e$ be incident on (collide with) a test

particle of charge and moving with a velocity particle of charge Z_2e and moving

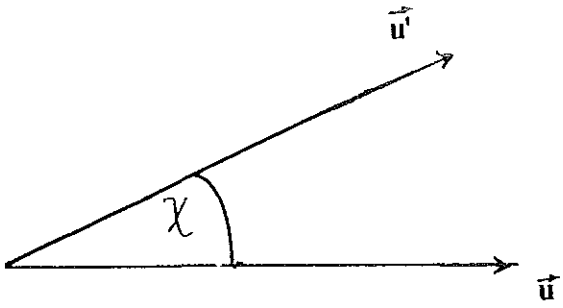

Fig 2.1 *Relation between the scattering angle and relative velocity.*

with a velocity $\vec{V}$.

Choosing the Z-axis to be the direction of the relative velocity of the interacting particles, the change in relative velocity (assuming elastic collision) that results from scattering is

$$\Delta u_z = u - u\cos\chi = 2u\sin^2(\tfrac{\chi}{2}) \qquad (2.2.1)$$

where χ is the scattering angle in the centre of mass system. The force that a single particle exerts on the test particle in an interval of time Δt is then

$$F_z = \frac{\Delta p_z}{\Delta t} = \frac{\mu \Delta u_z}{\Delta t} = \frac{2\mu u \sin^2(\frac{\chi}{2})}{\Delta t} \qquad (2.2.2)$$

where Δp_z is the change in momentum transferred, μ is the reduced mass of the

interacting particles. $\mu = \frac{m_e m_i}{m_e + m_i} \approx m_e$ where m_e and m_i are masses of the electron and ion respectively. For a total of $n u d\sigma(u) \Delta t$ interacting particles across a differential cross-section of $d\sigma(u)$ where n is the concentration (number density of particles), equation (2.2.2) will be

$$F_z = 2\mu u^2 n d\sigma(u)\sin^2(\tfrac{\chi}{2}) \qquad (2.2.3)$$

From the Rutherford scattering formula [Ref. 16], the cross-section is related to the distance of closest approach (impact parameter ρ) by

$$d\sigma(u) = \pi\, d(\rho^2) \tag{2.2.4}$$

with $\rho^2 = \frac{Z_1^2 Z_2^2 e^4}{\mu^2 u^4} \cot^2(\frac{\chi}{2})$

Then, equation (2.2.3) becomes

$$F_z = -\frac{4\pi n Z_1^2 Z_2^2 e^4}{\mu u^2} \{\frac{d(\sin\frac{\chi}{2})}{\sin\frac{\chi}{2}}\} \tag{2.2.5}$$

The total force is obtained by integrating equation (2.2.5) over the scattering angle χ from 0 to π.

$$F_z = -\frac{4\pi n Z_1^2 Z_2^2 e^4}{\mu u^2} \ln[\sin(\frac{\chi}{2})]_o^{\pi} \tag{2.2.6}$$

The integral diverges logarithmically at small angles and we therefore introduce a cut-off [Ref. 14, 17] at χ_{min} to obtain

$$F_z = \frac{4\pi n Z_1^2 Z_2^2 e^4}{\mu u^2} \ln[\sin(\frac{\chi_{min}}{2})] \tag{2.2.7}$$

The small angle (χ_{min}) deflection corresponds to scattering with very large impact parameters and they are related by

$$\chi_{min} = \frac{2 Z_1 Z_2 e^2}{\mu u^2 \rho_{max}} \tag{2.2.8}$$

The divergence arises from the long range nature of Coulomb force. This divergence is eliminated, however, when we take into account the shielding that arises from the polarization charge surrounding the test particle. The polarization screens the scattering particle and provides a natural cut-off on the maximum impact parameter of the order of [Ref. 17], a Debye length λ_d, and a value for the logarithm in equation (2.2.6) of

$$\ln[\sin(\frac{\chi}{2})]_{\chi_{min}}^{\pi} = -\ln(\rho_{max} \frac{\mu u^2}{Z_1 Z_2}) = \Lambda \tag{2.2.9}$$

and the total force on the test particle in vector form

$$\vec{F}(\vec{u}) = -\frac{4\pi n Z_1^2 Z_2^2 e^4}{\mu}\Lambda\frac{\vec{u}}{u^3} \qquad (2.2.10)$$

The quantity Λ is called Coulomb logarithm. The exact value of the stopping power (retarding force) can be found using the dielectric permitivity $[\varepsilon(\vec{k},\omega)]$ formalism of the plasma. For a Maxwellian plasma it has been found by I.Larkin [Ref. 18] and for a degenerate quantum plasma by D.G.Yakovlev and S.S.Kotelnikov [Ref. 19]. Since the Coulomb logarithm varies only slowly as a function of u, in this case, it is treated as a constant.

For particles of the plasma having a Maxwellian distribution $f(\vec{v'})$ the total force can be generalized [Ref. 20], as

$$\vec{F}(\vec{v}) = -\frac{4\pi n Z_1^2 Z_2^2 e^4}{\mu}\Lambda\int\frac{(\vec{v}-\vec{v}')}{\left|\vec{v}-\vec{v}'\right|^3}f(\vec{v})\,d\vec{v}' \qquad (2.2.11)$$

It is interesting to note here a formal similarity with electric field theory

$$\vec{E}(\vec{r}) = \int\frac{(\vec{r}-\vec{r}')}{\left|\vec{r}-\vec{r}'\right|^3}\rho(\vec{r}')\,d\vec{r}' \qquad (2.2.12)$$

where $\rho(\vec{r}')$ is the charge density of the plasma. The electric field at a point $\vec{r}$ for isotropic charge distribution can be found using Gauss theorem

$$E(r) = \frac{1}{r^2}\int\rho(\vec{r}')\,4\pi r'^2\,dr' \qquad (2.2.13)$$

In a similar way for a particle distributed in velocity space at a point $\vec{v}$, the force is found to be

$$F = -\frac{4\pi n Z_1^2 Z_2^2 e^4}{\mu}\Lambda\{\frac{1}{v^2}\int_0^v(\frac{m}{2\pi\Theta})^{3/2}\exp(-\frac{mv'^2}{2\Theta})\,4\pi v'^2 dv' \qquad (2.2.14)$$

where m is mass of the plasma particles (mainly electrons due to their small mass compared to that of the ions) and $(\frac{m}{2\pi\Theta})^{3/2} \exp(-\frac{mv^2}{2\Theta}$ is their Maxwellian distribution function, assuming a local equilibrium that $\Theta = \Theta(\vec{r})$, $n = n(\vec{r})$.

Letting $\eta = -\frac{4\pi n Z_1^2 Z_2^2 e^4}{\mu v^2}\Lambda$, $\alpha = \frac{m}{2\Theta}$ *and* $x = \sqrt{\alpha}\, v'$

$$F = \eta\{\frac{4\alpha^{3/2}}{\sqrt{\pi}}[-\frac{\partial}{\partial\alpha}(\frac{1}{\alpha}\int_0^{\sqrt{\alpha}\,v}\exp(-x^2)dx)]\} \qquad (2.2.15)$$

From which the value of the force is found to be

$$F = -\frac{4\pi n Z_1^2 Z_2^2 e^4}{\mu v^2}\Lambda\{erf(\sqrt{\frac{m}{2\Theta}}\,v) - \sqrt{\frac{2m}{\pi\Theta}}\,v\exp(-\frac{mv^2}{2\Theta}) \qquad (2.2.16)$$

where the function $\mathrm{erf}(\sqrt{\frac{m}{2\Theta}}\,v)$ [Ref. 22] is the error function of $(\sqrt{\frac{m}{2\Theta}}\,v)$. The stopping power coefficient as a function of the velocity of the test particle is then given by the ratio of equation (2.3.16) to the mass (m_i) of the test particle

$$a(v) = -\frac{4\pi n Z_1^2 Z_2^2 e^4}{m_i \mu v^2}\Lambda\{erf(\sqrt{\frac{m}{2\Theta}}\,v) - \sqrt{\frac{2m}{\pi\Theta}}\,v\exp(-\frac{mv^2}{2\Theta}) \qquad (2.2.17)$$

Since test particles are stopped mainly by electrons due to the smallness of mass of the electron compared to the mass of the ion $(m_i/m_e) >> 1$, the quantity $(m/2\Theta)^{1/2}$ can be taken as the inverse of the electron velocity v_e and μ as mass of the electron m_e.

Expanding the quantities in the bracket in equation (2.3.17) in Tailor series up to the second term of smallness of the ratio v/v_e, we obtain

$$a(v) = -\frac{16\sqrt{\pi}\, Z_1^2 Z_2^2 e^4}{3 m_i m_e}\Lambda(\frac{n_e v}{v_e^3}) \qquad (2.2.18)$$

which relates the stopping power coefficient to the concentration $n_{,e}$, the temperature Θ_e of the electron and velocity of the test particle v. i.e.

$$a(v) \propto \frac{n_e(r)}{\Theta_e^{3/2}(r)}\,v \qquad (2.2.19)$$

2.3 SOLUTION OF THE FOKKER-PLANCK EQUATION FOR A HOMOGENEOUS PLASMA

Many techniques have been used to solve the Fokker-Planck equation [Ref. 21]. In this section, we will try to obtain the solution of equation (2.1.3) using the Green function method when the plasma is taken to be spatially homogeneous with respect to the co-ordinate space.

For non-thermal test particles, the collision time is very short compared to the time taken by the plasma to expand or be compressed. Thus, for the formation of flux in the velocity space, it is possible to consider the process to be stationary. Under these conditions, we have to find the solution for the equation

$$\frac{\partial}{\partial \vec{v}}(\vec{a}(\vec{v})f) = S(\vec{v}) \qquad (2.3.1)$$

The friction coefficient $\vec{a}(\vec{v})$ is parallel to the velocity and its divergence has only radial component

$$\frac{\partial}{\partial v}(v^2 \left| \vec{a}(v) f \right|) = v^2 S \qquad (2.3.2)$$

Letting $v^2 f = q$ and $v^2 S = g$

$$\frac{\partial}{\partial v}(\left| \vec{a}(v) \right| q) = g \qquad (2.3.3)$$

It is possible to solve this equation easily using the ordinary integration method, but to be consistent with the method in the next section, the Green function method is used.

By the definition of the Green function, taking $\frac{\partial}{\partial v}(\left| \vec{a}(v) \right|)$ as a linear operator, the solution of equation (2.3.3) is

$$q(v) = \int_0^\infty g(v') G(v, v') dv' \qquad (2.3.4)$$

where G(v,v') is the Green function, v is the magnitude of the velocity of the test particle and v' is variable of integration (here it is considered to be the velocity of the test particle when it is created). With the above operator, the equation for the Green function is

$$\frac{\partial}{\partial v}\left(\left|\vec{a}(v)\right|\right) G(v, v') = \delta(v - v') \tag{2.3.5}$$

where $\delta(v - v')$ is the delta function, and the Green function here represents the distribution function for monochromatic source. Due to friction (collision),v is always less than v', hence

$$\frac{\partial}{\partial v}\left(\left|\vec{a}(v)\right|\right) G(v, v') = 0 \tag{2.3.6}$$

which gives for the Green function a value of

$$G(v,v') = \frac{constant}{\left|\vec{a}(v)\right|} \tag{2.3.7}$$

Using the boundary condition on equation (2.3.5) between $(v' - \varepsilon)$ and $(v' + \varepsilon)$ as the limit ε tends to zero and with the fact that $\vec{a}(\vec{v})$ is parallel to $\vec{v}$, we found the constant in the solution of the Green function to be unity. Therefore, the general form of the Green function is

$$G(v,v') = \begin{cases} 0 \text{ for } v' < v \\ \frac{1}{a(v)} \text{ for } v' > v \end{cases} \tag{2.3.8}$$

Then, the solution for equation (2.3.2) will have the form

$$v^2 f(v) = \int_0^v v'^2 s(v') G(v, v')\, dv' + \int_v^\infty v'^2 s(v) Gv, v')\, dv' \tag{2.3.9}$$

The first term on the right hand side of equation (2.3.9) is zero as v' cannot be less than v. Using the value of the source, S(v'), from section (1.3) which is Gaussian, we arrive at

$$f(v) = \frac{\Theta n_1 n_2}{2Mv^2 v_o^3 a(v)} \left(\frac{M}{2\pi\Theta}\right)^{3/2} \langle \sigma u \rangle \int_v^\infty v'^3 \exp[-\frac{M}{2\Theta}(v' - v_o)^2]\, dv' \qquad (2.3.10)$$

where v_0 is a constant velocity of the test particle when it is created. Letting v' - v_0 = x, we obtain

$$f(v) = \eta \alpha^{3/2} \int_{v-v_o}^\infty (x^3 + 3x v_o^2 + 3v_o x^2 + v_o^3)\, dx \qquad (2.3.11)$$

where $\eta = \frac{Tn_1 n_2}{2Mv^2 v_o^3 a(v)} \left(\frac{1}{\pi}\right)^{3/2} \langle \sigma u \rangle$ *and* $\alpha = \frac{M}{2\Theta}$. After carrying out the integral, f(v) is found to be

$$f(v) = \frac{\Theta n_1 n_2}{2Mv^2 v_o^3 a(v)} \left(\frac{M}{2\pi\Theta}\right)^{3/2} \langle \sigma u \rangle \left\{ \frac{\Theta}{M} \exp\left[-\frac{M}{2\Theta}(v - v_o)^2\right] \left[-\frac{2\Theta}{M} - v^2 + 5 v v_o - 6v_o^2\right] \right.$$

$$\left. \sqrt{\frac{2\pi\Theta}{M}} \left[\frac{v_o^3}{2} + \frac{3v_o\Theta}{2M}\right] erfc\left[\sqrt{\frac{M}{2\Theta}}(v - v_o)\right] \right\} \qquad (2.3.12)$$

where $\mathrm{erfc}[\sqrt{\frac{M}{2\Theta}}(v - v_o)]$ is [Ref. 22] the complementary error function of $[\sqrt{\frac{M}{2\Theta}}(v - v_o)]$.

2.4 THE GREEN FUNCTION OF THE FOKKER-PLANCK EQUATION FOR A NON-HOMOGENEOUS PLASMA

The systematic procedure is essentially the same as in section (2.3), but here a spatially non-homogeneous plasma is considered , i.e. the solution to the equation

$$\vec{v}\frac{\partial f}{\partial \vec{r}} + \frac{\partial}{\partial \vec{v}}(\vec{a}(\vec{v}, \vec{r})f) = S(\vec{v}, \vec{r}) \qquad (2.4.1)$$

is to be found.

where the process is taken to be stationary by the same reasoning as in the previous

section. The equation for the Green function with $\vec{v}\frac{\partial}{\partial \vec{r}} + \frac{\partial}{\partial \vec{v}}(\vec{a}(\vec{v}, \vec{r}))$ considered as a linear operator is

$$\vec{v}\frac{\partial G}{\partial \vec{r}} + \frac{\partial}{\partial \vec{v}}(\vec{a}(\vec{v}, \vec{r})G) = \delta(\vec{v} - \vec{v}')\delta(\vec{v} - \vec{r}') \qquad (2.4.2)$$

There is no term in the operator $\vec{v}\frac{\partial}{\partial \vec{r}} + \frac{\partial}{\partial \vec{v}}(\vec{a}(\vec{v}, \vec{r}))$ that changes the direction of the

velocity $\vec{v}$, because $\vec{a}$ is parallel to $\vec{v}$. Hence the Green function may be written as

$$G(\vec{v}, \vec{r}; \vec{v}', \vec{r}') = G(v, \vec{r}; v', \vec{r}')\ \delta(\vec{e}_v - \vec{e}_{v'}) \qquad (2.4.3)$$

where $\vec{e}_v$ and $\vec{e}_{v'}$ are unit vectors of the velocities. Choosing the Z-axis along the constant

direction of the velocity and using the fact that $\vec{a}(\vec{v})$ is parallel to $\vec{v}$

$$v\frac{\partial G}{\partial z} + \frac{1}{v}\frac{\partial}{\partial v}(v^2\left|\vec{a}(v, \vec{r})\right| G) = \frac{1}{v^2}\delta(v - v')\delta(\vec{r} - \vec{r}') \qquad (2.4.4)$$

where the divergence of $(\vec{v}, \vec{r})$ with respect to the velocity space is taken to have radial component only as it is along the Z-axis.

According to equation (2.2.19) in the stopping power coefficient $\vec{a}(v, \vec{r})$, it is possible to separate the variables $\vec{r}$ and v as $\left|\vec{a}(v, \vec{r})\right| = h(\vec{r})g(v) = h(z)g(v)$. Then it holds

$$\frac{1}{v}\frac{\partial G_1}{\partial z} + \frac{h(z)}{v^2}\frac{\partial}{\partial v}(G_1 g(v)) = \frac{1}{v^2}\delta(v - v')\,\delta(\vec{r} - \vec{r}') \qquad (2.4.5)$$

where $G_1(v, \vec{r}; v', \vec{r}') = v^2\, G(v, \vec{r}; v', \vec{r}')$. Again with the substitution $G_2 = g(v)\, G_1$

$$\frac{1}{h(z)}\frac{\partial G_2}{\partial z} + \frac{g(v)}{v}\frac{\partial G_2}{\partial v} = \frac{g(v)}{v h(z)}\delta(v - v')\,\delta(\vec{r} - \vec{r}') \qquad (2.4.6)$$

Using $Z = \int_{z'}^{z} h(z)\,dz$ *and* $V = \int_{v}^{v_o} \frac{v}{g(v)}\,dv$ for which $G_2(v, \vec{r}; v', \vec{r}') = 0$ when $V < 0$, we get

$$\frac{\partial G_2}{\partial Z} + \frac{\partial G_2}{\partial V} = \frac{\delta(v - v')}{v/g(v)}\frac{\delta(\vec{r} - \vec{r}')}{h(z)} \qquad (2.4.7)$$

Decomposing $\delta(\vec{r} - \vec{r}')$ into its parallel and perpendicular components (with respect to the constant direction of v), where the parallel component is the Z-component, we have

$$\delta(\vec{r} - \vec{r}') = \delta(\vec{r}_\perp - \vec{r}_\perp')\,\delta(z - z') \quad \text{and}$$

$$\frac{\partial G_2}{\partial Z} + \frac{\partial G_2}{\partial V} = \frac{\delta(v - v')}{v/g(v)}\frac{\delta(z - z')}{h(z)}\delta(\vec{r}_\perp - \vec{r}_\perp') \qquad (2.4.8)$$

Letting $G_2(v, \vec{r}; v', \vec{r}') = G_3(v, \vec{r}'; v, \vec{r}')\,\delta(\vec{r}_\perp' - \vec{r}_\perp')$ one can write

$$\frac{\partial G_3}{\partial Z} + \frac{\partial G_3}{\partial V} = \frac{\delta(v - v)}{v/g(v)}\frac{\delta(z - z)}{h(z)} \qquad (2.4.9)$$

It can be shown that $\frac{\delta(v-v')}{v/g(v)} = \delta(V)$ *and* $\frac{\delta(z-z')}{h(z)} = \delta(Z)$ so that

$$\frac{\partial G_3}{\partial Z} + \frac{\partial G_3}{\partial V} = \delta(Z)\,\delta(V) \tag{2.4.10}$$

Since v is always less than v′ due to friction, $\delta(V) = 0$. Therefore,

$$\frac{\partial G_3}{\partial Z} + \frac{\partial G_3}{\partial V} = 0 \tag{2.4.11}$$

The solution of this equation is an arbitrary function of the difference Z-V

$$G_3(Z, V) = \phi(Z - V) \tag{2.4.12}$$

By boundary condition, taking the integral of equation (2.4.10) over V between ε and -ε as the limit ε tends to zero, we obtain

$$G_3(Z, V) = \delta(Z) \tag{2.4.13}$$

From equations (2.4.12) and (2.4.13), the solution of the Green function $G_3(Z, V)$ is

$$G_3(Z, V) = \delta(Z - V) \tag{2.4.14}$$

This equation implies that if we have fixed the values of V, then Z is also fixed and the function $G_3(Z, V)$ shows the stopping of particles from a point source.

The physical meaning of the functions h(z) and g(v) can be found as follows. For a spherical plasma target, the concentration n and the temperature Θ of the plasma particles are assumed to be homogeneous, and as we have seen in section (2.2), the stopping power coefficient a(v,r) is linearly proportional to the velocity of the test particles. i.e. a(v,r) = (constant) (v). Also the stopping power coefficient is related to the stopping range $\lambda(\vec{r})$ by

$$\lambda(\vec{r}) = \int_0^{v_0} \frac{v}{a(v, \vec{r})}\, dv \tag{2.4.15}$$

where the lower limit of the integration indicates the velocity of the particle when it is stopped. Thus for the stopping range one can obtain

$$\lambda(\vec{r}) = \frac{v_o}{constant} \tag{2.4.16}$$

This gives a value for the constant to be $\frac{V_o}{\lambda(\vec{r})}$. Therefore,

$$a(v,z) = \frac{v\,v_o}{\lambda(z)} \tag{2.4.17}$$

from which $g(v) = v.v_0$ and $h(z) = \frac{1}{\lambda(z)}$. Thus h(z) can be interpreted as the reciprocal of the stopping range.

CHAPTER THREE

3. NUMERICAL SOLUTION OF THE FOKKER-PLANCK EQUATION

A recent powerful method to overcome physical problems for which experiments are difficult and also analytic theoretical treatments are complex is the method of computer simulation or computer modelling.

In this chapter the solution of Fokker-Planck equation (the distribution function $f(\vec{v}, \vec{r})$) is to be completed numerically which was partially carried out analytically in the foregoing chapter, and the non-equilibrium distribution of particles will be investigated.

The original Green function $G(\vec{v}, \vec{r}; \vec{v}', \vec{r}')$ in section (2.4) can be written as

$$G(\vec{v}, \vec{r}; \vec{v}', \vec{r}') = \frac{\delta(\vec{r}_1 - \vec{r}_1')\delta(\vec{e}_v - \vec{e}_{v'})}{v^2 g(v)} \delta(Z - V) \qquad (3.1)$$

Then the distribution function in the Fokker-Planck equation is

$$f(\vec{v}, \vec{r}) = \int G(\vec{v}, \vec{r}; \vec{v}', \vec{r}') \, S(\vec{v}', \vec{r}') \, d\vec{v}' \, d\vec{r}' \qquad (3.2)$$

the integral being over the velocity and the co-ordinate spaces. Since the gap between the velocity v_0 of the charged test particles at which they are created and their thermalization velocity v (their spreading) is much larger than the line width of the Gaussian distribution (which drops quickly) of the source, it is possible to consider the source to be proportional to the delta function. i.e.

$$S(v, r) = n_1(r) n_2(r) \langle \sigma u \rangle \frac{\delta(v - v_0)}{4\pi v^2} \qquad (3.3)$$

where $v_o = \sqrt{\frac{2Q}{m}}$, and Q is the heat of reaction (assuming isotropic emission of particles in the primary reaction).

Therefore, the distribution function in equation (3.2) is

$$f(\vec{v}, \vec{r}) = \int \frac{\delta(Z-V)\delta(\vec{r}_\perp - \vec{r}_\perp')\delta(\vec{e}_{v'} - \vec{e}_v)}{4\pi v^2 g(v)} n_1(\vec{r}') n_2(\vec{r}') \langle \sigma u \rangle \frac{\delta(v'-v_o)}{v'^2} d\vec{r}' \, d\vec{v}' \qquad (3.4)$$

Using spherical co-ordinates in the velocity space and cylindrical co-ordinates in the co-ordinate space, and taking the Z-axis to be the constant direction of motion

$$f(\vec{v}, \vec{r}) = \int \frac{\delta(Z-V)}{4\pi v^2 g(v)} n_1(z', \vec{r}_\perp) n_2(z', \vec{r}_\perp) \langle \sigma u \rangle \delta(v' - v_o) dv' \, dz' \qquad (3.5)$$

With the Jacobean transformation of z and Z

$$f(\vec{v}, \vec{r}) = \frac{\lambda(z')}{4\pi v^2 g(v)} n_1(z', \vec{r}_\perp) n_2(z', \vec{r}_\perp) \langle \sigma u \rangle \qquad (3.6)$$

where $z' = z'(r,v,\beta)$, must be found from the equation $\int_v^{v_o} \frac{v\,dv}{g(v)} = \int_{z'}^{z} \frac{dz}{\lambda(z)}$. i.e. the point at

which Z = V. Here β is the angle between the direction of motion of the test particle and the radial vector of this particle with the origin at the center of the spherical target.

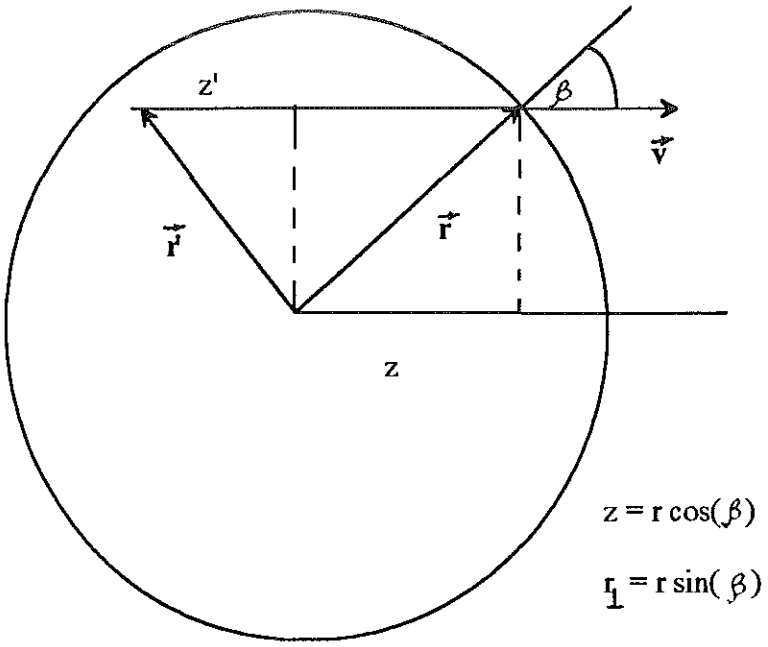

Fig. 3.1. *Motion of the test particle in a spherical target.*

Fig. 3.1. shows the motion of a test particle in a spherical target. r' is the point at which the particle is created and r is its current position relative to the centre of the target.

Knowledge of the current position r of the particle moving with a velocity $\vec{v}$ at an angle β at a point r permits us to know the point r' where it is created and hence the value of the distribution function.

The quantity $\langle \sigma u \rangle$ is an implicit function of the radius vector through the temperature. This can be shown as follows. Referring back to chapter one this average value is given by

$$\langle \sigma(u)\, u \rangle = \left(\frac{\mu}{2\pi\Theta}\right)^{3/2} \int \sigma(u)\, u \exp\left(-\frac{\mu u^2}{2\Theta}\right) u^2\, du\, d \qquad (3.7)$$

But the function $\sigma(u)$ [see, for e.g., Ref. 7], is given by

$$\sigma(u) = \frac{A}{u^2} \exp[-\frac{4\pi^2 z_1 z_2 e^2}{h u}] \qquad (3.8)$$

where A is considered as a constant for low energies. Then equation (3.7) becomes

$$\langle \sigma(u)\, u \rangle = 4\pi A (\frac{\mu}{2\pi\Theta})^{3/2} \int_0^\infty u \exp[-\frac{\mu u^2}{2\Theta} - \frac{4\pi^2 z_1 z_2 e^2}{h u}]\, d \qquad (3.9)$$

The quantity $y(u) = \frac{\mu u^2}{2\Theta} + \frac{\nu_c}{u}$, where $\nu_c = \frac{4\pi^2 z_1 z_2 e^2}{h}$, has minimum value at $u_{min} = [\frac{\nu_c \Theta}{\mu}]^{1/3}$. Expanding y(u) in Taylor series about u_{min}

$$y(u) \approx \frac{3}{2}[\frac{\mu \nu_c^2}{\Theta}]^{1/3} + \frac{3\mu}{2\Theta}[u - u_{min}] \qquad (3.10)$$

Substituting this value of y(u) into equation (3.9) and using the saddle-point method for a smooth function h(x) and a sharp function p(x) (see e.g. Fig. 3.2 below), the integral $\int h(x)\, p(x)\, dx$ [Ref. 23], can be approximated by $h(x) \int p(x)\, dx$, we obtain

$$\langle \sigma(u)\, u \rangle = \text{constant} \; \frac{\exp\left[-\frac{3}{2}(\frac{\mu \nu_c^2}{\Theta})^{1/3}\right]}{\Theta^{2/3}} \qquad (3.11)$$

Now coming back to equation (3.6), to have a flux of particles, we have to find points at which Z = V, i.e., we have to solve the equation

$$\int_{\nu}^{\nu_o} \frac{\nu\, d\nu}{g(\nu)} = \int_{z'}^{z} \frac{dz}{\lambda(z)} \qquad (3.12)$$

numerically using the procedures (algorithms) given in the following section.

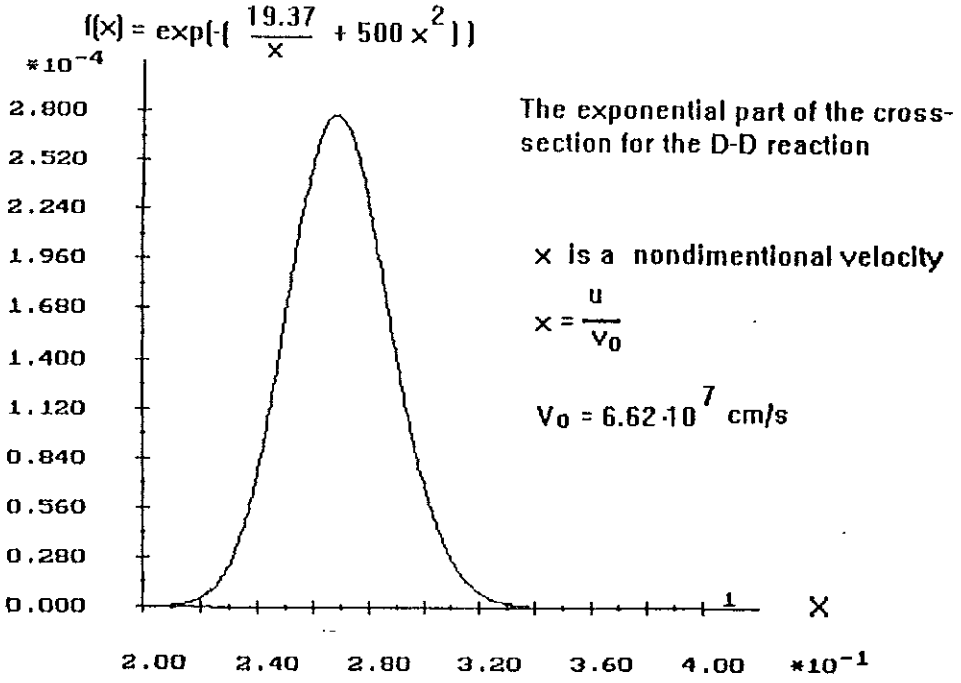

Fig. 3. *A schematic diagram showing the sharpness of the function* $\exp[-\frac{\mu u^2}{2\Theta} - \frac{4\pi^2 Z_1 Z_2 e^2}{hu}$, *the constant numbers used in the expression are values of the parametres for the reaction in equation (1.2.3)*

3.1 THE ALGORITHM OF THE PROGRAM FOR THE NUMERICAL SOLUTION

The structure of our program will be described by the following scheme.

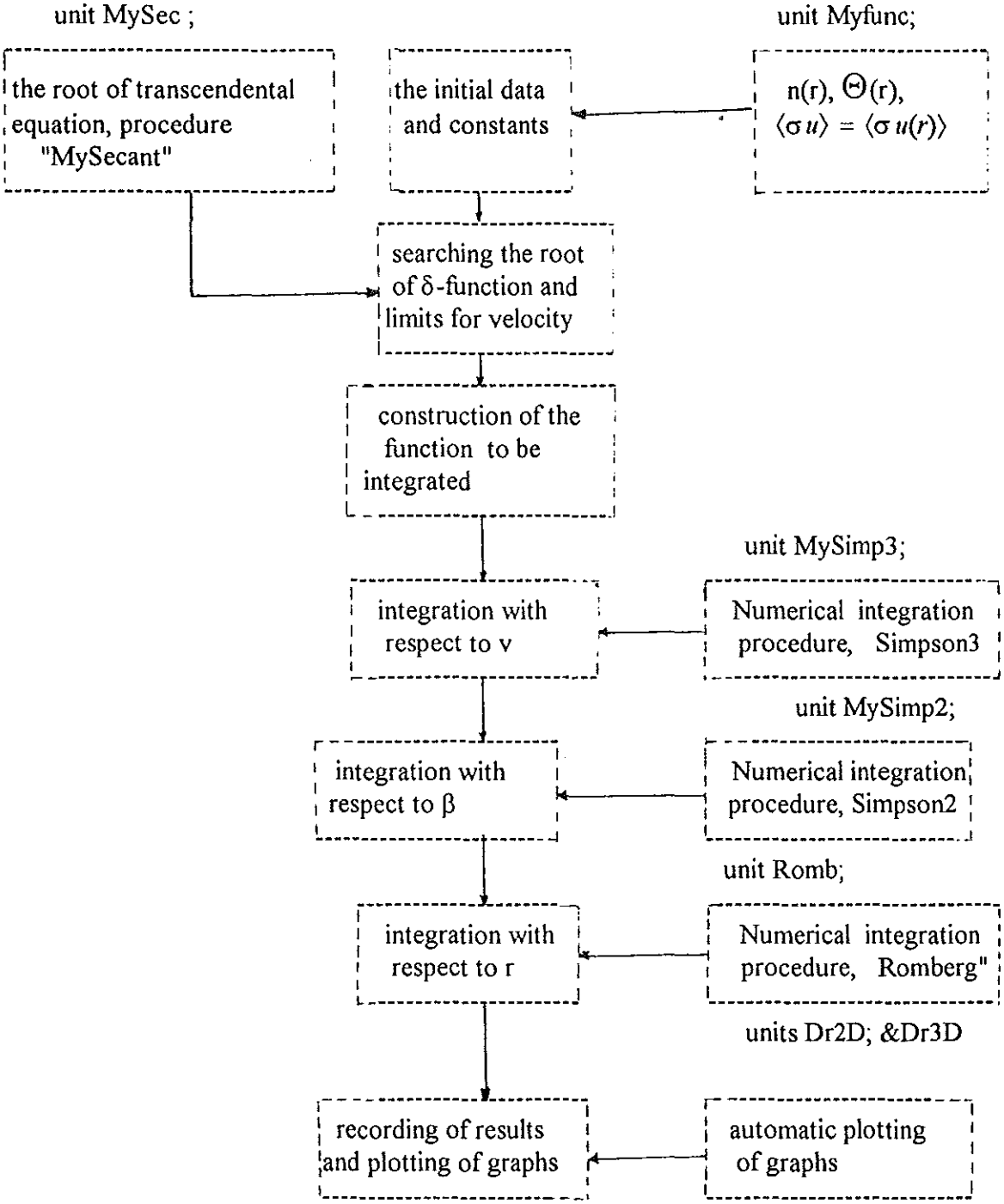

The program is provided with the initial data and values of the constants used in the equation to be solved. As shown in a table form (flow chart) above, it is nacessary to go via different sub-programs to solve the desired equation.

In addition to our own programs, one unit program the unit "Romb;" (Romberg method) from Turbo Pascal Numerical Methods Toolbox which were created by the Borland International, Inc., in 1986, 87 was used.

The unit program "Myfunc;" was created to determine the distribution of the concentration and the temperature in the compressed target and to find the distribution of the quantity $\langle \sigma u \rangle$ with respect to the radius. The temperature $\Theta(r)$ of the plasma is taken to be in the order of 10 keV at the center of the target and the concentration n(r) [Ref. 24], is a decaying function with respect to the radius of the target. Simple modification of this unit allows the ues of the program for the investigation of spectra with other models of distribution of concentration and temperature (see figures in section 3.2).

The other unit programs are the "Dr2D;" and "Dr3D;" which were created to provide procedures for drawing graphs of the required equation and to have a simultaneous graphic control during calculations. In using these unit programs, one has to specify the number of points (divisions) on the axes (the function to be plotted and its arguments). The scale for all of the axes is created automatically.

The MySec unit program was created to give procedures for finding real roots of a transcendental equation in one variable with a given specified initial interval for a single root. The procedure implements the method of the secant lines to find a single root of a function of four variables keeping the three constant. In our program, we used it to find the root of the δ-function (equation (2.4.13)) and know the limit of the velocity of the test particle (whether the particle comes to stop totally or it can leave the target with some minimum velocity v_{min}). The unit program has been tested on known transcendential equations.

The unit "Romb;" as it was created by the Borland International, Inc., was designed to provide procedures for performing numerical integration in one variable with the controlled tolerance. It approximates the given integral from the lower limit to upper limit of integration using the "Romberg" method. To carry out numerical integrations in two and three dimensions with respect to the dimensionless velocity x ($x = v/v_o$), the dimensionless radius r (r = radius/ $\lambda(0)$), where $\lambda(0)$ is the stopping range of a test particle at the center of the target) and the angle β between the velocity $\vec{v}$ of the test particle and its radius vector $\vec{r}$ from the center of the spherical target, we modified the standard Simpson procedure. The two and three dimensional integration is described by the units "MySim2" and "MySim3" respectively. These two units have been tested on functions for which analytical integration can be performed. The unit Romb is used to control the tolerance of the last integration and hence the total tolerance of calculation.

The main program is finally tested on uniform distribution of concentration of the plasma particles. We applied part of the program to calculate the spectra of charged particles from primary reaction (equation (1.1.2)), taking into account the energy loss due to Coulomb interaction with particles of the plasma.

3.2. THE RESULT OF DIGITAL SIMULATION OF THE DISTRIBUTION FUNCTION IN THE FOKKER-PLANCK EQUATION AND THE SPECTRUM OF FAST TRITON

Simulations of the distribution function and spectrum of charged test particle (triton)

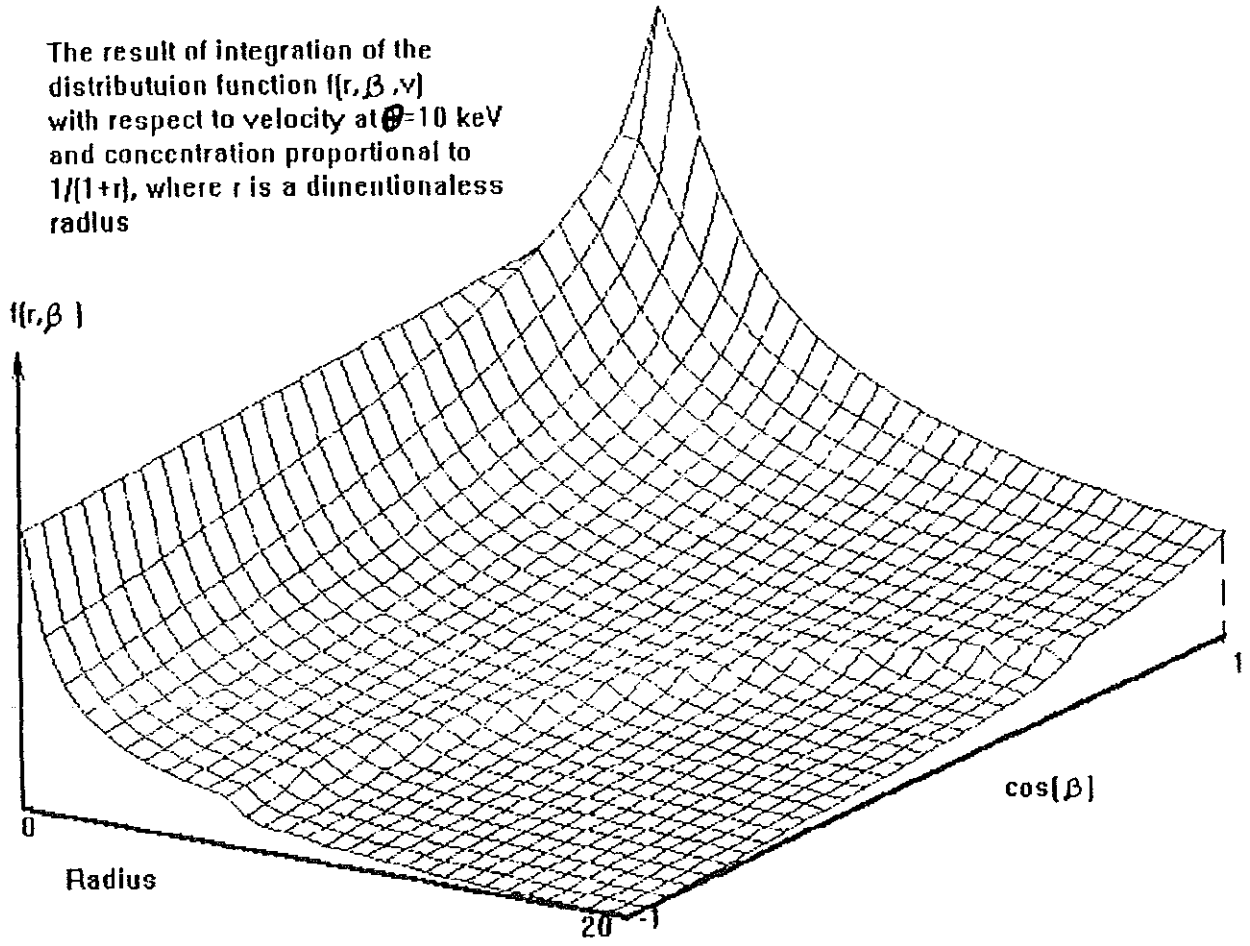

(a)

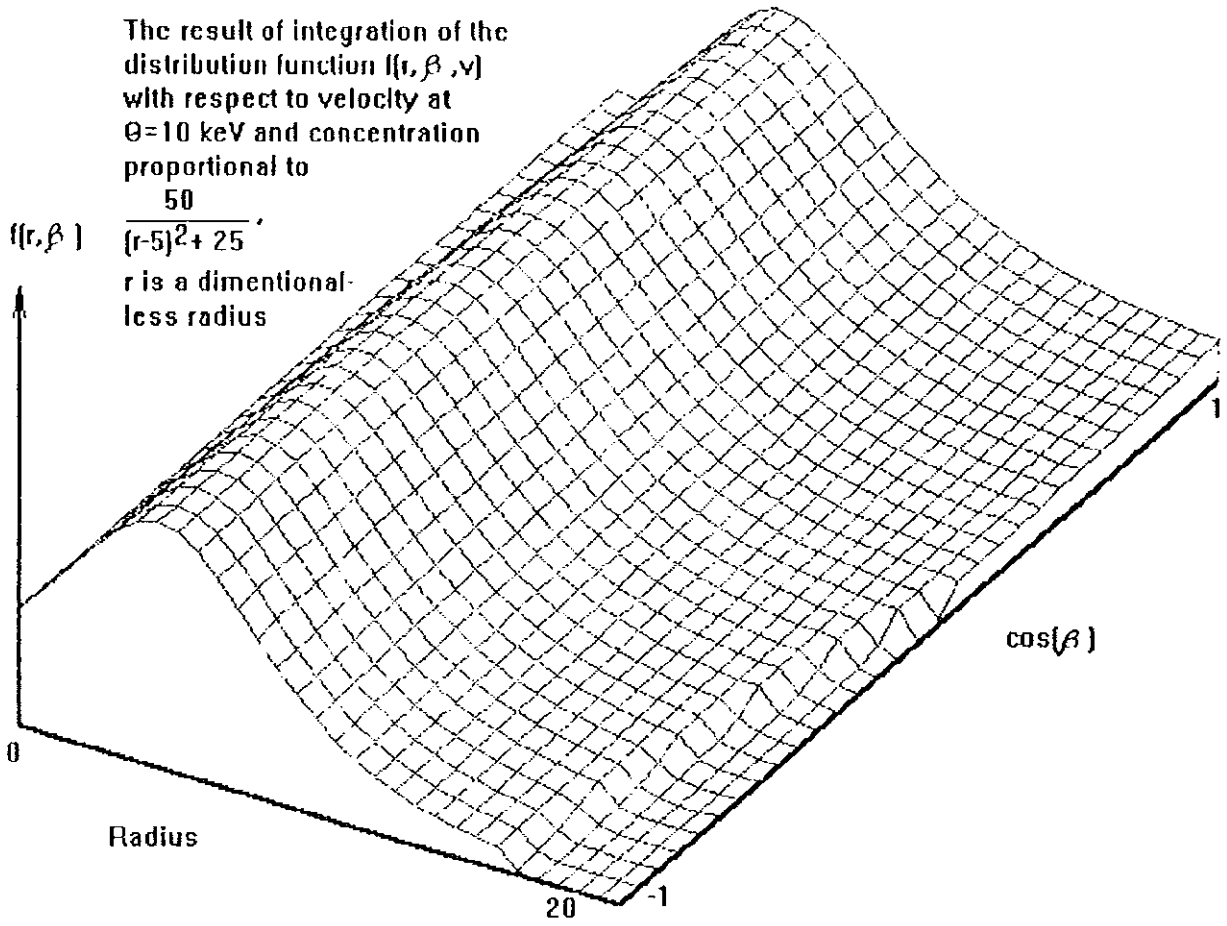

(b)

Fig. 3.2.1 *The distribution functions of fast tritons as a function of the distance from the center of the target (dimensionless radius) and the cosine of the angle between the direction of motion of the triton and the radius vector.*

have been carried out and the results are shown in Figs. 3.2.1 and 3.2.2. As it has been mentioned, the drag (friction) experienced by a charged particle traveling through, often changes its distribution function. To find the shape of this function, we took a test particle

(triton) with velocity lying between v_{min} and v_o, where v_o is the velocity when it is created and v_{min} is its velocity for which the Fokker-Planck equation is valid.

From the physical point of view the distribution function at the centre can not be a function of the anglulr orientation of the particle. This is observed in this case too as can be seen from the Figs. The distribution function in Fig. 3.2.1a has maximum at a point a little displaced from the center. This can be explained as :

i. The distribution function is inversely proportional to the velocity (see the multiplier g(v) in the solution for the Fokker-Planck equation).
ii. Since the distribution function is integrated numerically with respect to the velocity of the test particle, due to the reason in (i) the main contribution to the distribution function comes from the minimum value (lower limit) of the velocity.

But a particle cannot be stopped at a point where it is created and a particle that is created in the center will lose its velocity at a point displaced from the center approximately equal to the stopping range (in our case it is normalized to unity at the center). Thus the function should have a maximum displaced from the centre of the target a distance approximately equal to the minimum value of the stopping range.

In general, the function decreases with respect to both arguments radius and $\cos\beta$. The decrease with respect to the angle beta is due to the fact that a particle with negative value of $\cos\beta$ comes from the external region of the target where the concentration of the source of the test particle is smaller, while for those positive values it comes from the point where there are more sources for the creation of the particles.

The distribution function is smoothly decreasing from the origin to a point approximately half of the radius of the target and beyond this point, but it decreases sharply at this point. This effect is the result of the increase of v_{min} due to the large value of the stopping range

($\lambda \propto \frac{1}{n}$) and all particles cannot be stopped with v_{min} within the target. i.e. due to relation between the stopping range and concentration and thus the radius, for some points of the target, the stopping range becomes outside of the target. This means that there are particles which come from the external region of the target where the concentration is small.

The physical reasoning for the behavior of the distribution function in Fig. 3.2.1b is essentially the same as in Fig. 3.2.1a. But the maximum point of the function lies at a point where the concentration of the sources of the particles is maximum (at r = 5). Because of the small value of the local stopping range in comparison to the former one. i.e. a particle can be stopped near a point where it is created, hence there is no displacement between the maximum of the distribution function and concentration of plasma particles.

The same effect of changing of the smoothness of the function appears here too. But now, due to a small value of the local stopping range, this effect is shifted towards the boundary and there is no constraints on v_{min} for a particle that comes from the center ($\beta \approx 0$). It exists only for value of β near $\pi/2$.

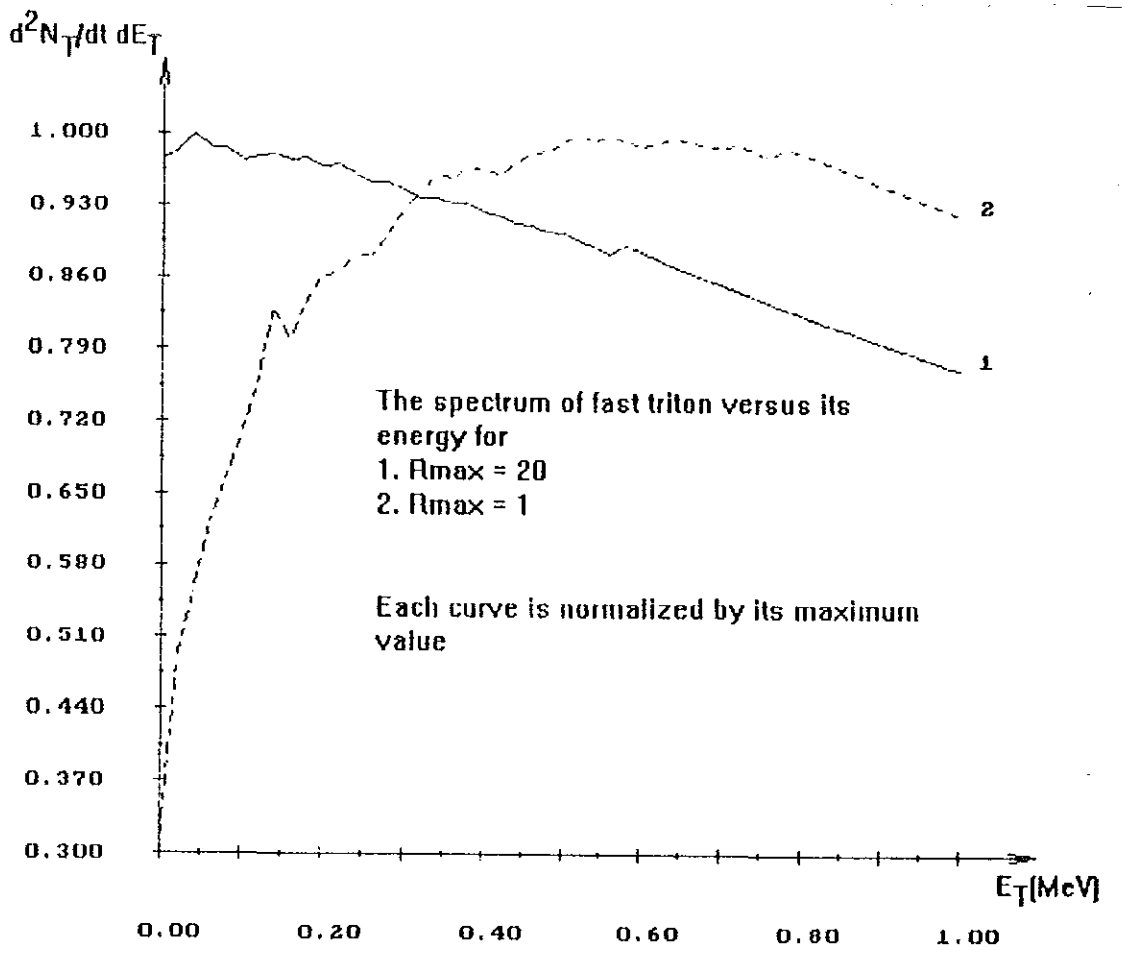

Fig. 3.2.2 *The energy spectrum of fast triton for*
1. $R_{max} = 20$
2. $R_{max} = 1$

The spectrum of test particles (fast tritons) can be found by the integration of the boundary value of the distribution function with respect to the angle β from 0 to π/2 (the normal cömponent of the flux of particles)

$$\frac{dN_T}{dt\,dE_T} = 4\pi\,\nu R_{\max}^2 \int_0^1 f(R_{\max}, \cos\beta, \nu)\ \cos\beta\, d(\cos\beta) \qquad (3.2.1)$$

For the two curves indicated in the figure, the concentration of plasma particles is taken to be proportional to 1/(1 + r), but for different values of the boundary.

For such calculations, we obtained curves like those in Fig. 3.2.2. The two curves represent the spectra of fast tritons from reactio (1.1.2) obtained for two different sizes of the target.

Curve 1 is the spectrum for which the dimensionless maximum radius of the target is 20. Since the minimum value of the stopping range is unity (at the centre of the target), it is small compared to the size of the target for this value of the radius. Therefore, the energy (velocity) of the triton has all the possible values from thermalization to 1 MeV (v_o) to be stopped within the target and due to the inverse proportionality of the distribution function to the velocity,the spectrum is found to have a maximum near the minimum value the energy.

Curve 2 represents the spectrum for which the maximum dimensionless radiu is unity. This is also the point at which the stopping range is minimum at the centre of the target , so that there is no possibility for a particle to be stopped within the target with the energy down the thermalization velocity.

From the inverse proportionality of the distribution function to the velocity of the particle, in principle, the spectrum should have a maximum near the minimum value of energy. But as described above, there is no such minimum value of velocity in this case. The absence of a particle with minimum velocity on one hand and the dependence of the distribution function on this minimum value on the other hand bring a tendency of equilibrium between the two in the spectrum. Hence the spectrum has a smooth maximum.

Our results are qualitatively in agreement with the results in Refs. 30 and 31 which were found by the Monte Carlo simulation method. To calculate the spectra numerically, the unit program " Romberg " was not used where there is a control of tolerance. That is why some small numerical fluctuations appeared in the spectra.

CHAPTER FOUR

4. THE NUMERICAL SIMULATION OF THE SPECTRUM OF PHOTONS PRODUCED FROM THE SECONDARY FUSION REACTIONS IN A NON-HOMOGENEOUS PLASMA

As it has been discussed earlier the distribution function of fast (test) charged particles in a plasma is non-Maxwellian. This in tern brings a change in the spectrum of particles from its Gaussian form. To see this let us take the reaction (1.2.3) in which a triton with birth energy 1 MeV from equation (1.1.2) reacts with deuteron in the target which is assumed to be at rest compared to the incident triton.

$$D + D \rightarrow p + T$$

$$T^{fast} + D \rightarrow {}^5H_e + \gamma \qquad Q = 16.62 \text{ MeV} \qquad (4.1)$$

The reaction rate for the photons produced is then

$$\frac{dN_\gamma}{dt} = \int f_T(\vec{r}, \vec{v})\, n_D(\vec{r})\, v\, (\frac{d\sigma}{d\Omega_\gamma})\, d\Omega_\gamma\, d\vec{v} \qquad (4.2)$$

where $\vec{v}$ is velocity of the triton (the relative velocity of the two interacting particles is taken to be the same as the triton velocity), $f_T(\vec{v}, \vec{r})$ is the distribution function of the fast triton as given in equation (3.6).

In a similar way as in section (1.4), the spectrum of the photons produced can be found as

$$\frac{d^2N_\gamma}{dt\, dE_\gamma} = \int f_T(\vec{v}, \vec{r})\, n_D(\vec{r})\, v\, (\frac{d\sigma}{d\Omega_\gamma})\, \delta[E_\gamma - E'_\gamma(1 + \frac{m_T}{M}(v/c)\cos\theta)]\, d\Omega_\gamma\, d\vec{v} \qquad (4.3)$$

where M = m_D + m_T and the centre of mass velocity is $\vec{V} = \frac{m_T}{M}\vec{v}$ since deuteron is assumed to be at rest compared to the triton.

Using the value of the distribution function of tritons from equation (3.6), we obtain

$$\frac{d^2N_\gamma}{dt\,dE_\gamma} = \int_{-1}^{1}\int_{v_{min}}^{v_o} \frac{n_D^2(z')n_T(\vec{r})}{4\pi g(v)}\lambda(z')\langle\sigma u\rangle v\,\delta[E_\gamma - E'_\gamma(1+\frac{m_T}{M}(v/c)\cos\theta)]$$

$$(\frac{d\sigma}{d\Omega_\gamma})\,2\pi\,d(-\cos\theta)\,dv \qquad (4.4)$$

The angular distribution of photons produced in a low energy reaction is [Ref. 8], proportional to $P_{11}^2 = \sin^2\theta$, where P_{11} is the associate Legendre Polynomials (so called l-scattering) and the reaction (scattering) differential cross-section is given by

$$\frac{d\sigma}{d\Omega_\gamma} = \frac{A\sin^2\theta}{v^2}\exp[-\frac{4\pi^2 Z_1 Z_2 e^2}{hv}] \qquad (4.5)$$

where A is a constant (or very smooth function of v) to be found from the interpolation of the experimental data. Then the spectrum becomes

$$\frac{1}{2v_o}\int_{-1}^{1}\int_{v_{min}}^{v_o} n_D^2(z')n_T(\vec{r})\lambda(z')\langle\sigma u\rangle\sigma_{DT\gamma}(1-\cos^2\theta)\ \times$$

$$\delta[E_\gamma - E'_\gamma(1+\frac{m_T}{M}(v/c)\cos\theta)]\,d(-\cos\theta)\,dv \qquad (4.6)$$

By the property of delta function, this can be written as

$$\frac{d^2N\gamma}{dt\,dE_\gamma} = \frac{1}{2v_o}\int_0^\infty n_D^2(z')n_T(\vec{r})\,\lambda(z')\langle\sigma u\rangle\sigma_{DT\gamma}\{1-[(\frac{E_\gamma}{E'_\gamma}-1)\frac{M}{m_T}(v/c)]^2\}$$

$$\frac{M}{m_T|E'_\gamma(v/c)|}\xi(E_\gamma, v)\,dv \qquad (4.7)$$

where the quantity $\xi(E_\gamma, v)$ is used simply to control (adlust) the value(range) of cosθ for the simulation.

$$\xi(E_\gamma, v) = \begin{cases} o \text{ if } \left| \left\{ \frac{E_\gamma}{(Q + \frac{\mu v^2}{2})} - 1 \right\} \frac{M}{m_T} c/v \right| > 1 \\ 1 \text{ if } \left| \left\{ \frac{E_\gamma}{(Q + \frac{\mu v^2}{2})} - 1 \right\} \frac{M}{m_T} c/v \right| \leq 1 \end{cases} \qquad (4.8)$$

Note here that the energy of the photon in the centre of mass system is $E'_\gamma = Q + \frac{\mu v^2}{2}$. Therefore, the spectrum of the photon produced to be integrated numerically is

$$\frac{d^2N_\gamma}{dt\,dE_\gamma} = \frac{1}{2v_o} \int_{v_{min}}^{v_o} n_D^2(z')\, n_T(\vec{r})\, \lambda(z') \langle \sigma u \rangle \sigma_{DT\gamma} \{1 - [(\frac{E_\gamma}{(Q + \frac{\mu v^2}{2})} - 1) \frac{M}{m_T} (v/c)]^2\}$$

$$(\frac{M}{m_T}) \frac{\xi(E_\gamma, v)}{Q + \frac{\mu v^2}{2}} (c/v)\, dv \qquad (4.9)$$

4.1. THE RESULT OF THE NUMERICAL SIMULATION OF THE PRIMARY AND SECONDARY SPECTRA OF PHOTONS

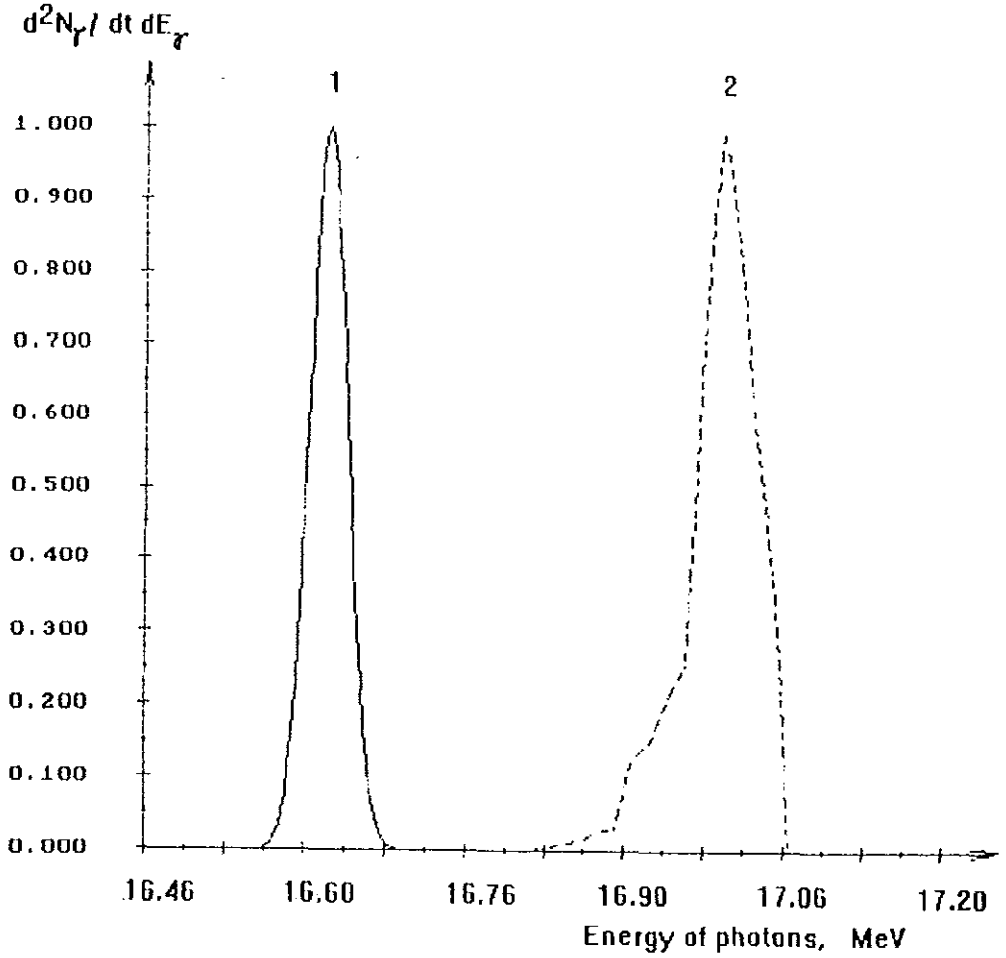

Fig. 4.1. *The spectra of primary photons (eqution (1.1.4), curve 1) and secondary photons (equation (1.2.3.), curve 2). Each spetrum is normalized to its maximum value.*

The spectrum of the primary photons is calculated based on equation (1.4.11) with maximum value at $E_\gamma = Q = 16.63\,MeV$ and the with at the temperature of 10 keV.

The maximum value of the spectrum for the secondary photons is displaced from the primary by the relative energy of the fast triton (0.4 MeV). The maximum point of the

spectrum has the tendency to be displaced towards the maximum energy due to the absence of acceleration as the velocity of the test particle is decreasing (the initial increasing of the spectrum is due to the behaviour of the the exponential term in the cross-section of the secondary reaction and the sharp falling is due the distribution function, i.e. due to the absence of a particle with velocity greater than v_o).

4.2. ESTIMATION OF THE YIELD AND POSSIBILITIES FOR THE DETECTION OF SECONDARY PHOTONS

The yield (Y_γ) of photons (number of photons per unit time) in the secondary reaction can be estimated by using the primary DT neutron yield. The yield ratio of the secondary photons to the primary DT neutrons [Ref. 26], is proportional to the ratio of $\langle \sigma u \rangle$ values of the reactions.

$$\frac{Y_\gamma}{Y_n} = \frac{\langle \sigma u \rangle_{DD}}{\langle \sigma u \rangle_{DT}} \sigma_{DT\gamma} v_T n_D \tau \qquad (4.2.1)$$

where $\sigma_{DT\gamma}$ is the DTγ cross-section in equation (1.2.3) and τ is the confinement time. The ratio $\frac{\langle \sigma u \rangle_{DD}}{\langle \sigma u \rangle_{DT}}$ [Ref. 25] is 1/30 for large interval of temperature (10 keV) and $\sigma_{DT\gamma}$ is [Ref 28] is10^{-27} cm^2 .

As currently reported in Ref. 27, the yield of the primary DT neutron is ranging from 10^{14} to 10^{16} for a pulse of laser light. Therefore, with values of $v_T = 8.10^7$ cm/s, the confinement time $\tau = 10^{-9}$ s and the primary DT neutron concentration nD = 10^{24} cm^{-3} , the yield of secondary photons is

$$Y_\gamma \approx 2.7 \times 10^8 \; to \; 2.7 \times 10^8 \qquad (4.2.2)$$

The photons produced in the target can, in principle transfer their energy to the plasma particles when they interact with this particles. For the totally ionized plasma, the two main

effects of photon interaction with the plasma particles are Compton scattering and pair production. The total scattering cross-section in this absorption (absorption in a sence here is absorption from a fixed energy) of photons by matter (plasma particles) is the sum of the cross-sections due to the two effects. But as compared to the Compton scattering [Ref. 29], the cross-section for the pair production is very small ($\sigma_c = 10^3 \sigma_{e^-e^+}$) . Thus, the absoption of photons comes mostly from Compton effect and the absorption length is given by

$$L = \frac{1}{n_D \sigma_c} \approx 1\, cm \qquad (4.2.3)$$

The value of the absorption length is much greater than the dimension of the compressed target which is usually in the order of 10^{-3} cm. This implies that ther is no transformation of the energy of photons due to the interaction with the particles of the plasma. Hence, using usual detector equipment copious photons can be detected in such fusion reactions.

CONCLUSION

It has been attempted to give a review of the calculation of the spectra of primary fusion products, neutrons and to investigate the spectra of primary photons. The solution for the Fokker-Planck equation has been carried out partially analytically for a non-homogeneous plasma and with the help of this analytical solution, an algorithm for the numerical simulation of the distribution function and the spectra of the primary and secondary fusion reaction products (tritons and Photons) has been developed.

The comparison of the theoretical prediction of the spectra for each model of the state of a target with experiment can be used as a test for the model of the distribution of plasma particles. The results are qualitatively in agreement with the results obtained by the Monte Carlo simulation method.

It was stated in Ref. 5 that detailed measurment (knowledge) of the neutron yield can be used to estimate the absolute photon yield per pulse of laser light. Using this idea in the present work it has been found that for the deutron concentration $10^{24}\,cm^{-3}$ and test particle velocity in the order of $10^{7}\,cm/s$, the neutron yield is six order of magnitude greater than that of the photons.

Appendix

The purpose of this appendix is to present the original text of the programs we created for the numerical simulation. The appendix consists of six unit programs and the main program called Takele.

The unit programs listing follows.

1. The text of the unit program Myfunc (to determine the distribution of the quantities in the compressed target). We created this unit to organize together all the functions and parameters used for the description of the state of the target and specific values of constants related to the primary and secondary reactions (here equations (1.1.2) and (1.2.3)).

```
unit Myfunc;
interface
 const
 Rmax:real = 20;
      Alpha:real = 10.8169;    {- Alpha = 3/2 (μv_c^2/T_o)^1/3                -}

      Emax:real = 17.0754;     {- Emax = (Q + μv_o^2/2) (1 + v_o /c)          -}
      Emin:real  = 16.5856;    {- Emin = Q (1- v_o/c)                         -}
c-over-vo:real = 625
Q: real = 16.63;                {- the heat of D-T-Gamma reaction -}
function  N(x:real):real;
function  T(X:real):real;
 function  Lambda(x:real):real;
function Rate_DD(x:real):real;
function Cross_section_TDGamma(x:real):real;

implementation
 {--------------------------}
 function  N(x:real):real; begin N:=1/(x+1) end;
{--------------------------}
function  T(x:real):real;
begin T: = 1  end;
 {--------------------------}
 function  Lambda(x:real):real;
begin Lambda:=exp(3/2*ln(T(x)))/N(x) end;
 {--------------------------}
 function Rate_DD(x:real):real;
 var Arg:real;
```

```
 begin Arg:=Alpha*(exp(-1/3*ln(T(X)) -1));
if Arg>100 then Rate_DD:=0 else Rate_DD:=exp(-Arg)/(exp(2/3*ln(T(x))));
 end;
{-------------------------------------}
 function Cross_section_TDGamma(cosTeta:real;x:real):real;
var Arg:real; begin if x=0 then Cross_section_TDGamma:=0
else begin Arg:=16.76/x;          {- Vc/Vo = 16.76- }
  if Arg>100 then Cross_section_TDGamma:=0
   else Cross_section_TDGamma:=(1-sqr(cosTeta))*exp(-Arg)/sqr(x)
end;
end;
{-------------------------------------}
 end.
```

2. The interface and the comment parts of the unit program Dr2D for plotting graphs. This program is created to have a simultaneous graphic control of all the programs during calculations.

```
unit Dr2D;
{- This  unit  provides procedure for drawing  of  the  curves .     -}
 {---------------------------------------------------------------------}
 interface      uses  Dos, Crt, Graph;
 const         ArraySize = 400;
 TNNearlyZero  = 1E-015;
  XDensityTouch  = 10;  { XDensityTouch  must be  < 21          -}
  YDensityTouch  = 10;  { YDensityTouch  must be  < 21          -}
 LeftDeviationForYAxis = 120;
BottomDeviationForXAxis = 60;
 ShiftTextFromYAxis     = 75;
WidthTouchXYAxis       = 3;
 type
          Float   = real;
MyNumPoints   = array [1..5] of integer;
Vector            = array [1..ArraySize] of  float;
Matrix            = array [1..ArraySize,0..9] of float;

 procedure PLOT2D (     NumPlots : integer ;
                      ArrayNumPoints : MyNumPoints ;
                         ScaleXAxis     : Float;
                         ScaleYAxis     : Float;
                                 var G : matrix ) ;
{---------------------------------------------------------------------}
{-  This  program draws the plots of functions.                    -}
```

```
{-  The parameters of procedure PLOT2D                                -}
{-------------------------------------------------------------------}
{-     NumPlots  - number of functions F(J,X),  J=1,2..NumPlots,     -}
{-              X - argument, NumPlots < = 5.                        -}
{-                                                                   -}
{- ArrayNumPoints  - array of number points of F[J,X] function,      -}
{-              J=1,2..NumPlots,   NumPlots < = 5.                   -}
{-              ArrayNumPoints = array [1..NumPlots] of integer.     -}
{-                                                                   -}
{-              ArrayNumPoints[1]  = NumPoints1 - the number         -}
{-              of the points of the 1 function,                     -}
{-              ArrayNumPoints[2]  = NumPoints2  - the number        -}
{-              of the points of the 2 function,                     -}
{-              ..................................................   -}
{-              ArrayNumPoints[5]  = NumPoints5  - the number        -}
{-              of the points of the 5 function.                     -}
{-            ------------------------------------   -}
{- ScaleXAxis    - the scale of the X axis,                          -}
{-                 0.45  < ScaleXAxis <= 1 .                         -}
{-                                                                   -}
{- ScaleYAxis    - the scale of the Y axis,                          -}
{-                 0.45 <  ScaleYAxis  <= 1.                         -}
{-                                                                   -}
{-      var G  -  G[I,J] = array [1..TNArraySize,0..9] of data.      -}
{-                                                                   -}
{-              X1[I] = G[I,0]  -array values of X1 arguments,       -}
{-            F(1,X[I]) = G[I,1]  -array values of F1 function,      -}
{-                          I=1,2...NumPoints1.                      -}
{-                                                                   -}
{-              X2[I] = G[I,2]  -array values of X2 arguments,       -}
{-            F(2,X[I]) = G[I,3]  -array values of F2 function .     -}
{-                          I=1,2...NumPoints2.                      -}
{-              ..................................................   -}
{-              X5[I] = G[I,8]  -array values of X5 arguments,       -}
{-            F(5,X[I]) = G[I,9]  -array values of F5 function.      -}
{-                          I=1,2...NumPoints5.                      -}
{-                                                                   -}
{-------------------------------------------------------------------}
```

3. The interface and the comment parts of the unit Romb. We have taken this program from Turbo Pascal Numerical Method Toolbox to perform one dimensional integration of the function of one variable with controlled tolerance.

```
unit Romb;
{- Turbo Pascal Numerical Methods Toolbox                                    -}
{- This unit provides procedures for performing numerical integration -}

interface

procedure Romberg(LowerLimit : Float;
                  UpperLimit : Float;
                  Tolerance  : Float;
                  MaxIter    : integer;
                 var Integral : Float;
                  var Iter    : integer;
                 var Error    : byte;
                  FuncPtr     : Pointer);
{-------------------------------------------------------------------------}
{-                                                                        -}
{-   Input: LowerLimit, UpperLimit, Tolerance, MaxIter                    -}
{-  Output: Integral, Iter, Error                                         -}
{-                                                                        -}
{- Purpose: Given a function, TNTargetF(X), this procedure approximates   -}
{-          the integral of TNTargetF from LowerLimit to UpperLimit       -}
{-          using the Romberg method.                                     -}
{-                                                                        -}
{- User-defined Functions: TNTargetF(X : real) : real;                    -}
{-                                                                        -}
{-  Global Variables:  LowerLimit : real;   Lower limit of integration    -}
{-                     UpperLimit : real;   Upper limit of integration    -}
{-                      Tolerance : real;   Tolerance in answer           -}
{-                      MaxIter   : integer; Maximum number of iterations -}
{-                       Integral : real;   Value of the integral of      -}
{-                                  TNTargetF over the given              -}
{-                                  interval                              -}
{-                Iter     : integer; Number of iterations                -}
{-                Error    : byte;   Flags if something goes              -}
{-                                  wrong                                 -}
{-                                                                        -}
{-        Errors:  0: No errors                                           -}
{-                 1: Tolerance <= 0                                      -}
{-                 2: MaxIter <= 0                                        -}
{-                 3: Iter > MaxIter                                      -}
{-------------------------------------------------------------------------}
```

4. The text of the unit MySimp2 for the integration of functions of two variables. This unit program is used to carry out integrations of functions of two variables to be described in the main program following a known Simpson method.

```
unit MySim2;
 interface
 var Z,Y:real;
type
    Func_of_2=function(Y,X:real):real;
Float = real;  {- 6 byte real, no math chip required-}
const
     TNArraySize = 50;            { Size of the vectors }
type
  TNvector = array[0..TNArraySize] of Float;
procedure Simpson2(LowerLimit   : Float;
                           UpperLimit   : Float;
                          NumIntervals : integer;
                         var Integral     : Float;
                            var Error     : byte;
                                Myfunc: Func_of_2);
{-------------------------------------------------------------------------}



implementation
{$F+}
procedure Simpson2{(LowerLimit  : Float;
                           UpperLimit   : Float;
                          NumIntervals : integer;
                         var Integral     : Float;
                          var Error       : byte;
                            MyFunc       : Func_of_2)};
var
  Spacing : Float;          { Size of each subinterval }
     Point : Float;           { Midway point of each interval }
  OddSum, EvenSum : Float;  { Sums of values over odd numbered }
                                { and even numbered subintervals }
  LimitsValue : Float;       { Sum of values at the endpoints }
       Interval : integer;       { Counter }
begin { procedure Simpson }
    if NumIntervals <= 0 then
      Error := 1
   else
     begin
```

```
        Spacing := (UpperLimit - LowerLimit) / (2 * NumIntervals);
        Point := LowerLimit;
        OddSum := 0;
        EvenSum := 0;
        for Interval := 1 to 2*NumIntervals - 1 do
        begin
          Point := Point + Spacing;
          if Odd(Interval) then
            OddSum := OddSum + MyFunc(Y,Point)
         else
           EvenSum := EvenSum + MyFunc(Y,Point);
      end;
     LimitsValue := MyFunc(Y,UpperLimit) +
                    MyFunc(Y,LowerLimit);
     Integral := Spacing * (LimitsValue + 2 * EvenSum + 4 * OddSum) / 3;
   end;
end; { procedure Simpson2 }
end.
```

5. The text of the unit MySimp3 for the integration of functions of three variables. The procedure in this unit program is essentially the same as in MySim2 above, but here it is used for functions of three variables.

```
unit MySim3;
 interface var Z,Y:real;
 type  Func_of_3 = function(Z,Y,X:real):real;
Float = real;   { 6 byte real, no math chip required }
const  TNArraySize = 50;            { Size of the vectors }
type  TNvector = array[0..TNArraySize] of Float;
{-------------------------------------------------------------------------}
 procedure Simpson3(LowerLimit   : Float;
                    UpperLimit   : Float;
                    NumIntervals : integer;
                   var Integral     : Float;
                        var Error : byte;
                        Myfunc  : Func_of_3);
{-------------------------------------------------------------------------}
implementation
{$F+}
procedure Simpson3{(LowerLimit  : Float;
                     UpperLimit   : Float;
                    NumIntervals : integer;
                    var Integral     : Float;
```

```
                        var Error      : byte;
                         MyFunc      : Func_of_3)};
var  Spacing : Float;          { Size of each subinterval }
 Point : Float;           { Midway point of each interval }
 OddSum, EvenSum : Float;   { Sums of values over odd numbered }
                { and even numbered subintervals }
LimitsValue : Float;      { Sum of values at the endpoints }
 Interval : integer;      { Counter }
begin { procedure Simpson }
 if NumIntervals <= 0 then
  Error := 1  else
   begin
    Spacing := (UpperLimit - LowerLimit) / (2 * NumIntervals);
     Point := LowerLimit;
    OddSum := 0;
    EvenSum := 0;
  for Interval := 1 to 2*NumIntervals - 1 do
     begin
    Point := Point + Spacing;
     if Odd(Interval) then
     OddSum := OddSum + MyFunc(Z,Y,Point)
   else
    EvenSum := EvenSum + MyFunc(Z,Y,Point);
   end;
   LimitsValue := MyFunc(Z,Y,UpperLimit) +   MyFunc(Z,Y,LowerLimit);
    Integral := Spacing * (LimitsValue + 2 * EvenSum + 4 * OddSum) / 3;
   end;
end; { procedure Simpson3 }
end.
```

6. The unit program Mysec for finding the root of the function of four variables with respect to the fourth variable.

```
unit MySec;
interface
type func=function(Radius, cosBeta, V,x:real):real;
var Radius, cosBeta, V: real;
procedure Mysecant(Gess1,Gess2:real;Tolerance:real;Myfunc:func;
                                                    var root:real;
                                              var Value:real);
implementation
```

```
procedure Mysecant(Gess1,Gess2:real;Tolerance:real;Myfunc:func;
                                                    var root:real;
                                                var Value:real);

var x1,y1,x2,y2:real;
        x0,Y0:real;


procedure Secant(x1,y1,x2,y2:real; var x0:real;
                                    var y0:real);
    var Alpha:real;
    begin  Alpha:=(y2-y1)/(x2-x1);    x0:=x1-y1/Alpha;
     y0:=Myfunc(Radius, cosBeta, V, x0) end;
begin
 x1:=Gess1; x2:=Gess2; y1:=Myfunc(Radius, cosBeta, V,x1);
 y2:=Myfunc(Radius, cosBeta, V,x2);
if abs(y0)<Toleranse then begin root :=x0; value:= y0 end;
begin x1:=Gess1; x2:=Gess2;
 y1:=Myfunc(Radius,CosBeta,V,x1); y2:=Myfunc(Radius,CosBeta,V,x2);
if abs(y1)<Toleranse then begin root :=x1; value:= y1 end;
if abs(y2)<Toleranse then begin root :=x2; value:= y2 end;
 if y1*y2>0 then begin writeLn('Error in Gess1 and Gess2');readLn;halt(1) end;
if (y1>Tolerance) and (y2>Tolerance) and (y0> Tolerance) then
repeat
Secant(x1,y1,x2,y2,x0,y0);
 if (y1*y0)<=0 then begin y2:=y0; x2:=x0 end
                else if (y2*y0)<0 then
                            begin y1:=y0; x1:=x0 end
                    else begin writeln('Error in Secant'); readln; halt(1) end;
 if abs(y0)<Tolerance then begin root:=x0; Value:=y0 end;
until abs(y0)<Tolerance;
 end;
 end.
```

7. The main program for numerical simulation. In this program, we described the functions to be integrated. Parts of this program can be used to calculate the spectra and rates of charged particles produced in primary reactions.

```
program takele;
 {$M 65520,0,655360}
 {$F+}
 uses crt,Romb,Mysim3,Mysim2,Mysec,Dr2d,Myfunc;
 const MaxIter:integer=1000;
     Tolerance:real=10e-4;
```

```
    Intervals:integer=15;
 var
  Egamma:real;
  Error:byte;
 i:integer;
  StepforEnergy:real;
  G:matrix;
  ArrayNumPoints:MyNumPoints;
  Spect:real;
  outfile:text;
  Iter:integer;
 {-----------------------------------------}
 function Lambda1(Radius, CosBeta,U:real):real;
 var arg:real;
begin arg:=sqr(Radius)*(1-sqr(CosBeta))+sqr(U); if arg<0 then arg:=0;
Lambda1:=1/(Lambda(sqrt(arg)));
 end;
{-------------------------------------------------}
 function Root_of_deltafunc(Radius,cosBeta,V,Zprime:real):real;
 var UpperLimit:real;
   RadSqr:real;
   Integral:real;
begin {-function Root_of_deltafunc-}
 Upperlimit:=Radius*cosBeta;
  MySim3.Z:=Radius; Mysim3.Y:=cosBeta;  Error:=0;
 Simpson3(Zprime, Upperlimit, Intervals,Integral, Error,Lambda1);
Root_of_deltafunc:=1-V-Integral;
 end; {-function Root_of_deltafunc-}
 {-------------------------------------------------}
procedure Limit_for_V( Radius,cosBeta:real;var Vmin:real);
 var Upperlimit, LowLimit:real;
   Integral:real;
 begin {-procedure Limit_for_V-}
 LowLimit:=-sqrt( sqr(Rmax) -sqr(Radius)*(1-sqr(cosBeta)) );
 UpperLimit:=Radius*cosBeta;
 if LowLimit>=UpperLimit then Vmin:=1;
 MySim3.Z:=Radius; MySim3.Y:=cosBeta; Error:=0;
 Simpson3(LowLimit, Upperlimit, Intervals, Integral, Error,Lambda1);
 if Integral>=1 then Vmin:=0
else Vmin:=1-Integral;
end; {-procedure Limit_for_V-}
 {-----------------------------------------}
function RadBetaV(Radius, CosBeta,V:real):real;
var  Gess1,Gess2:real;
```

```
    Zprime,Value:real;
    Vmin,IntMax:real;
    ValueofCos:real;
    arg:real;
    Spr:integer;
function CosTeta(V:real):real;
  var Value:real;
 begin   if V=0 then CosTeta:=0
  else CosTeta:=(Egamma/(Q+2/5*sqr(v))-1)*C_over_Vo/V;
end;
function Spring(CosBeta:real):integer;
begin if abs(CosBeta)<=1 then Spring:=1 else Spring:=0
end;
begin Gess2:=Radius*CosBeta;
Gess1:=-sqrt(sqr(Rmax) - sqr(Radius)*(1-sqr(CosBeta)));
ValueofCos:=CosTeta(V);
Spr:=Spring(ValueofCos);
if Spr=0 then RadBetaV:=0
else begin if (Gess1>=Gess2) and (V<>1)
then RadBetaV:=0;
if (Gess1=Gess2) and (V=1)
 then begin arg:=Radius;
 RadBetaV:= Lambda(arg)*n(radius)*sqr(n(arg))*Rate_DD(arg)*  (1-sqr(ValueofCos))*
     Cross_section_TDgamma(V)/(Q+2/5*sqr(V)) end;
Limit_for_V(Radius,CosBeta,Vmin);
if V<Vmin then RadBetaV:=0;
if abs(Gess2-Gess1)<Tolerance
then
begin
arg:=Gess1;  RadBetaV:= Lambda(arg)*n(radius)*sqr(n(arg))*Rate_DD(arg)*
(1-sqr(ValueofCos))*  Cross_section_TDgamma(V)/(Q+2/5*sqr(V));
end;
if (abs(Gess2-Gess1)>Tolerance) and (V>=Vmin)
then
begin Mysec.Radius:=Radius; Mysec.CosBeta:=CosBeta; Mysec.V:=V;
Mysecant4(Gess1,Gess2, Tolerance,Root_of_Deltafunc,Zprime,Value);
arg:=sqrt( sqr(Zprime) + sqr(Radius)*(1-sqr(CosBeta)) );
if arg>=Rmax then RadBetaV:=0 else
 RadBetaV:= Lambda(arg)*n(radius)*sqr(n(arg))*Rate_DD(arg)*  (1-sqr(ValueofCos))*
     Cross_section_TDgamma(V)/(Q+2/5*sqr(V));
end; if abs(Zprime)>Rmax then RadBetaV:=0; end; end;
{-------------------------------------------------------------------}
function RadCosBeta (Radius,CosBeta:real):real;
var Vmin,Integral:real;
```

```
begin Limit_for_V( Radius,cosBeta, Vmin);
 Error:=0; MySim3.Z:=Radius; MySim3.Y:=CosBeta;
Simpson3(Vmin,1,10,Integral,Error,RadBetaV);
 RadCosBeta:=Integral;
 end;
{-------------------------------------------------------}
function Rad(Radius:real):real;
 var Integral:real;
 begin MySim2.Y:=Radius;
 Error:=0;
 Simpson2(-1,1,Intervals,Integral,Error,RadCosBeta);
Rad:=Integral*sqr(Radius);
end;
{-------------------------------------------------------}
begin  {-Main-}
 clrscr;
 Assign(outfile,'C:\tp\kotel\specgamm.dat');
 append(outfile);
 Egamma:=17.0572475;
 Romberg(0,Rmax,Tolerance,MaxIter,Spect,Iter,Error,@Rad);
 writeLn(Egamma,'  ',Spect);
 writeLn(outfile,Egamma,'  ',Spect); close(outfile);
 writeLn(' end of program');
readLn;
 end. {-end of the program-}
```

References

1. J. R. Roth, *Introduction to Fusion Energy*. Ibis Publishing. Charlottesville, Virginia, 1986.
2. K. Mukhin, *Experimental Nuclear Physics, vol.1*. Mir Publishers, Moscow, 1987.
3. M. D. Cable, *J. Appl. Phys.* **60** (1986) 3068.
4. W. Slivinsky et al, *Phys. Rev. Lett.* **35** (1975) 1083
5. S. S. Kotelnikov and E. A. Choban, *Sov. Phys. Tech. Phys.* **25** (1980) 910
6. Y. Setuhara et al, *Laser and Particle Beams* **8** (1990) 609
7. D. D. Clayton, *Principles of Stellar evolution and Nucleosynthesis*. McGraw-Hill, Inc., New York, 1968.
8. Landau and Lifshitz, *Quantum Mechanics*. Pergamon Press Ltd., London-Paris, 1958.
9. E. Zauderer, *Partial Differential Equations of Applied Mathematics*. John Willey & Sons, Inc., New York, 1986.
10. X. Z. Yan et al, *Phys. Rev.*, A **32** (1985) 1785.
11. C. K. Li and R. D. Petrasso, *Phys. Rev. Lett.* **70** (1993) 3059.
12. S. Ichimaru, *Basic Principles of Plasma Physics*. W. A. Benjamin, Inc., Canada, 1973.
13. C. K. Li and R. D. Petresso, *Phys. Rev. Lett.* **70** (1993) 3063.
14. M. N. Rosenbluth et al, *Phys. Rev.* **107** (1957) 1.
15. R. F. Post, *Nuclear fusion* **27** (1987) 1636.
16. J. B. Marion, *Classical Dynamics of Particles and Systems*. Academic Press, Inc., Florida, 1970.
17. R. S. Cohn et al, *Phys. Rev.* **80** (1950) 230.
18. I. Larkin, *Sov. Phys.* [JETP **10** (1960) 285, see, Ref. 19].
19. D. G. Yakovlev and S. S. Kotelnikov, *Sov. Phys.* [JETP **57** (1983) 781].
20. C. L. Longmire, *Elementary Plasma Physics*. John Willey & sons, Inc., New York, 1963.
21. P. Resibois and M. De Leener, *Classical Kinetic Theory of Fluids*. John Willey & sons, Inc., New York, 1977.
22. M. Abramowitz and I. A. Stegun, *Handbook of Mathematical Functions with Formulas, Graphs and Mathematical Tables*. Dove Publication Inc., New York, 1965.

23. A. G. Sveshnikov and Tikhonov, *The Theory of Functions of a Complex Variable*. Mir Publishers, Moscow, 1978.

24. H. Hora, *Plasma at High Temperature and Density.* Springer- Verlag, Berlin Heidenberg, New York, 1991.

25. K. A. Bruckner and S. Jorna. *Rev. Mod. Phys.* **46** (1974) 325.

26. G. M. Griffiths et al. *Can. J. Phys.* **41** (1963) 724.

27. H. Hora and G. H. Miley, *Laser interaction and related plasma phenomena.* Plenum press, New York. 1986.

28. V. N. Bezotosnyi et al. *Sov. J.Nuc. Phys.* **10** (1970) 127.

29. A. I. Akhiezer & V. B. Bersteskii. *Quantum Electrodynamics,* Interscince publishers, New York, 1965.

30. E. G. Gamalii et al. *JETP Lett.* **21** (1975)70.

31. S. Yu. Guskov et al, *Kvantovaya Electron.* (Kiev) **2** (1975) 2315.